UiO : Department of Informatics
University of Oslo

Hybrid Control of a Semi-Autonomous Ultrasound Robot

Combined Remote Force Feedback Control and Internal Force Control

John Ketil Willoch

Master's Thesis Spring 2017

Hybrid Control of a Semi-Autonomous Ultrasound Robot

John Ketil Willoch

May 7, 2017

Abstract

A new hybrid position-force control method has been implemented for a robotic system for use in ultrasound examinations. The hybrid controller combines an external force feedback position controller, with an internal compliance force controller. The hybrid controller makes use of a pedal to turn the compliance force controller on and off. This allows for a fluid workflow as you can turn the compliance force controller on and off whenever the need arises.

First we introduce the current robot system, and make a few improvements to the force feedback haptic controller. Then the implementation of the hybrid controller is presented, followed by system experiments. The experiments ensure that the real-time requirements of the system are met. They also measure the response of the new hybrid controller, compared to the old control methods. A qualitative user study is then performed, to gauge whether or not the hybrid controller feels like an improvement to the system for the operator.

The results from the system testing show that the real-time requirements are still upheld. Unfortunately the bandwidth response, and transparency of the new hybrid controller is worse than what we hoped. It is concluded that it does work as intended, but the individual parts of the hybrid controller need some improvements. The compliance force controller's bandwidth needs to achieve a better response bandwidth, and the force feedback haptic control would benefit from better transparency results.

Even with these shortcomings the user studies show that the hybrid controller is an improvement over the old control method when using the system.

Contents

List of Figures

List of Tables

Acknowledgements

This thesis is written as part of a project developed in partnership with the Intervention Center at Oslo University Hospital. I would first like to thank my primary thesis advisor Ole Jacob Elle, Section Manager for Technology Research at the Intervention Center. Without him, writing this thesis would not have been possible. Another thanks goes out to my secondary advisor Kyrre Harald Glette, Associate Professor at the Research Group for Robotics and Intelligent Systems at the University of Oslo. His weekly meetings continuously helped drive the work forward, and kept me on track with what needed to be done.

I would also like to give special thanks to Kim Mathiassen, scientist at the Norwegian Defence Research Establishment. His help has been paramount in properly understanding the previously developed system, as well as implementing new solutions.

Chapter 1

Introduction

When people get ill, they often have to travel from their local communities to find the expertise or medical equipment needed to meet their medical ailments. This is a natural cause of having bigger facilities, and more experienced staff at the centralized hospitals. While lack of medical equipment is hard to do something about, modern technology may allow for a lack of expertise to no longer be a problem. By the use of teleoperation a patient may receive specialist healthcare at their primary healthcare station.

One of the ongoing research projects at the Intervention Center at Oslo University Hospital is using robots to perform semi-automated ultrasound diagnostics. The goal is to be able to use a master-slave system with haptic feedback to perform the diagnostics. Radiologist have to exert a certain static force when performing an examination. Often this force has to be applied in awkward positions. This may end up causing the radiologist to develop musculoskeletal disorders [1] such as carpal tunnel syndrome [2]. By using a 6 degrees of freedom controlling device with haptic feedback, it will be possible to limit the amount of stress put on the radiologist. By scaling the feedback forces on the master controller a radiologist would still be able to feel what the slave system is doing, without having to apply too much force himself. A so called master-slave system is one where the the slave is controlled by a master controller. In this case the slave is a UR-5 Robot, and the master controller is a Phantom Omni haptic device. With such a system it is also possible to make the orientation of the slave system relative to the master controller, thus allowing the operator to avoid working in awkward angles.

This master-slave system opens up such possibilities of remote controlled diagnostics as mentioned above. In this thesis, however, the system will be implemented on a localized master-slave setup. This thesis builds upon the PhD-study of Kim Mathiassen. The research will encompass safety limitations within the Haptic software, and the creation of a hybrid position-force controller. This hybrid controller will enable the radiologist to find the appropriate pressure for a clear ultrasound image, and engage a dynamic force controller to keep said pressure. In doing so the radiologist can focus on other tasks, such as finding the right rotation or position for the image, or simply talking and explaining the image to the patient without worrying about the image changing.

1.1 Goals of the System

Even now there are ongoing discussions about robot systems being used in clinical work [3]. One of the main issues is often the lack of any sort of haptic feedback, and the challenges present in introducing such a system. The challenges often occur in ways of an unstable system, or simply a poorly integrated one. Even when the Da Vinci Surgical System, which is being used for Minimally Invasive Surgery (MIS) was introduced, it lacked

any sort of haptic feedback [4]. Surgeons using the system has voiced their opinion that haptic feedback integration could improve the performance. Research by Bethea et al. [5] proves this theory, and has shown that using haptic feedback can greatly improve certain tasks with the Da Vinci system, such as tying a knot with the correct force applied, which can be a crucial part of the surgery.

While our system will not be used for MIS we still want to close the gap between the robot and the controller by using a bilateral haptic feedback system. This will increase the patients safety, and possibly comfort as there will be a far smaller risk of the radiologist applying too much pressure, as compared to using a non-haptic feedback system. With a correct implementation it will also allow the radiologist to get a more precise feel for what the robot arm is doing and how it is positioned, both of which is crucial in ultrasound examinations.

Another great benefit of such a system will be the amount of force the radiologist has to exert. In a normal ultrasound examination the radiologist has to apply a lot of static pressure, often in weird angles. As mentioned this can cause a variety of symptoms, such as Carpal Tunnel Syndrome and shoulder pains. With our system it is possible to greatly limit the amount of force the radiologist have to apply, as well as remove the strain of applying said force at awkward angles.

While the system will be running on a local computer, and with a predetermined haptic controller hardware [6], it is developed in such a way that it can be controlled remotely. The haptic controll system is also made in a way which makes the hardware interchangeable. As long as the haptic controller has 6 DOF, any controller should be usable [7]. This opens the possibility of remote assistance in a ultrasound examination in cases where you want a second opinion from an expert off-site, even if he does not have the exact same haptic hardware. It also allows for remote controlled examinations in general.

The robot is commercially available, and relatively low cost for a robotic system. It also comes with the benefit of automating certain tasks during an ultrasound assisted operation, or examination. Another goal of the system is to be able to seamlessly allow the robot arm to take control of certain tasks, such as force control and positional control. When the radiologist finds the right position, and pressure he can give those tasks over to an automated system which will dynamically keep both the pressure and the position at the set points, relative to the patient. While the robot arm takes care of the pressure the surgeon may for example rotate the ultrasound probe around the point of contact. Or even simpler, the radiologist can lock only one or two axis in order to keep the pressure, while still moving the probe around an area on the patients body. All of these functions can ease the work for the radiologist by combining both robotic, and human

strengths. With the two buttons on the phantom controller these functions can be made to work intuitively, in such a way that the radiologist can jump back and forth between the different "modes" to readjust a previously applied pressure, and still keep the newly acquired rotation. Whether or not more buttons are necessary in order to realise such an implementation remains to be seen.

Below is a short list about exactly what we wish to achieve.

- Improve the current implementation of the haptic controller.
- Implement a new hybrid controller for the system, capable of:
  - Combining internal force control with external haptic control.
  - Allow for movement and rotation, while still dynamically maintaining the applied force in a given direction.
  - Achieving a good workflow, with a fluid way to turn the force control on and off.

Chapter 2

Background

2.1 Suspended or Handheld Robots

The use of teleoperation is far from being a new concept. Teleoperators for use in extracorporal ultrasound diagnostics specifically have been researched and developed for close to two decades [8]. One example is SYRTECH [9] which was developed by Gourdon et al. in 1999. This system is held in place over the patient, while the teleoperator performs the operation. There have been clinically successful tests done with a robot such as this. An example is the ESTELE system (Expert System for TELe Echography) [10] shown in figure 2.1. In this system an on site paramedic is needed in order to place the lightweight robot into the right position. The positioning of the robot is based on instructions given by the expert sitting at a remote location.

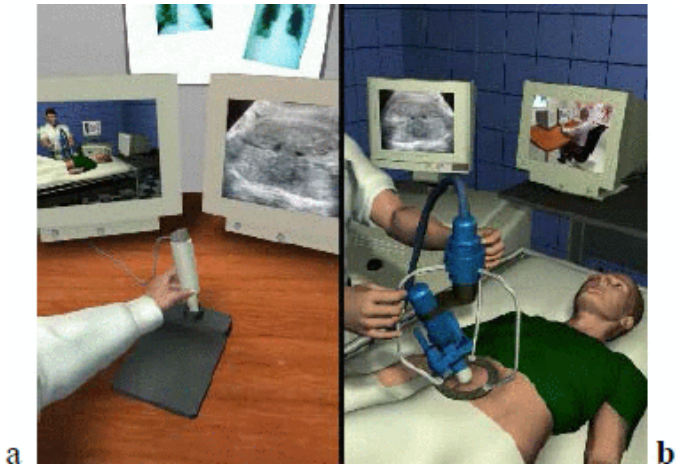

Figure 2.1: A graphical render of the ESTELE system as seen from the controller (a), and patients (b) perspective [10]

The expert would then be able to change the angle of the probe by using his controller. With such a system it is still necessary to communicate clearly with the paramedic in order to get the necessary pressure and position for a correct echo graphic image. While the test showed promising results the probe and robot had to be repositioned more often than during a conventional echography. The echography process also took longer using this method.

Neither of these two robotic systems had any kind of force sensors. For the SYRTECH robot it was pre-determined by a doctor that it would not be necessary, while in the ESTELE system this has not been discussed. Both of the above examples were robots that had to be held in place above the patient.

Courreges et al. have also developed OTELO [11] which can be seen as a third generation of the SYRTECH system. This also has to be placed above the patient. There are more examples of robots like this, such as one

proposed by Vilchis et al. which would be spanned from the four corners of the patient's bed, leaving it hanging in place above the patient [12].

2.2 Robotic Arm System

One example that differs in design is the robot developed by Salcudean et al. [1]. This is a robot arm that would be placed next to the patient in a way that would allow it to reach the patient within its workspace. This removes the need for a paramedic to initially position the robot. Another example is a robotic system proposed by Pierrot et al. [13]. In this system they first made use of an existing robot arm, *PA-10*, produced by Mitsubishi. This however lacked the security features necessary for use on patients. Therefore the robotic system HIPPOCRATE was developed. This robot implements force control. Among other things this would allow for a constant force to be applied towards the patient, in order to uphold contact with the patient's skin. It also incorporates a redundant system which makes the robot safe for use on patients, and around people. It does, however, lack any kind of force feedback, which would allow for the controller to feel the pressure applied by the robotic arm. And the option to apply such a haptic feedback system is not discussed.

Da Vinci Surgical System One of the more successful robotic arm systems used in a medical setting is the da Vinci surgical system made by Intuitive Surgical [14]. This system has been successfully used in both minimally invasive surgery operations, and normal open operations. It features a multitude of tools for most kinds of surgery, controlled by an external controller set-up using a 3D HD vision system to get a clear and magnified view of the operation from the surgeons controlling console. The system does not have any integrated force feedback, but Shimachi et al. proposes an adapter for the system, allowing for contact force sensing [15]. They conclude that the adapter is functional, though that the weight might make the robot arms unbalanced.

2.3 Haptic Feedback Systems

Haptic-based ultrasound training systems, such as HUTES [16], have been developed. This makes use of a Phantom haptic device and modular software to simulate the feedback. The feedback is simplified and static in this example, as there were no deformable virtual volume sets developed to simulate an actual patient.

Another example of a haptic-based system have been developed by Riccardo Antonello et al. [17]. This system also makes use of an actual robot arm controlled through a master-slave system where a Phantom device is used on the master side. The robotic arm holds a proximity sensor and moves according to the Phantom device, while simultaneously

Figure 2.2: The PHANTOM Omni device [6].

giving force feedback to the Phantom. For this system, which uses a proximity sensor, the force feedback would ensure that the master can feel when the robot arm reaches its desired range from its target. The haptic force feedback when approaching the target is generated to simulate an elastic virtual constraint placed above the surface to be inspected. In other words, no actual contact between the surface and the probe is made. This does however prove the concept, and it should be possible to replace the proximity sensor with a force sensor and get similar results when actually touching an elastic entity, or patient.

Normally for haptic devices, and teleoperation in general, a PID controller is used. Sansanayuth et al. [18] proposes another method. They also use the Phantom Omni device for their research, but instead of setting up a robot arm as a slave, they use a second Phantom device, similar to the first one. The main difference in their research is the use of inverse dynamic control, instead of a conventional PID controller. Inverse dynamic control is a special kind of feedback linearization, which according to their paper clearly improves the performance of the teleoperated system. While the inverse dynamics controller is worth looking into, we will be using a normal PID controller for our research. Mainly because the current system is already built around this control algorithm, and also because it is a well-known standard as far as controllers go, making it easier to implement and tune.

2.4 Force-Reflecting

One problem with force feedback systems is the backlash when the slave hits an object. A violent recoiling of the master occurs, which causes issues for the operator when attempting to make stable contact with the environment. Solutions to this problem include canceling the induced master motion [19], or reflecting a projection of the force feedback from the environment [20]. An example of such a backlash can be seen in figure 2.3. The figure shows the measured force and the position in z-direction on the slave site. As seen roughly 15 seconds into the measurements, force is introduced. This is sent back to the master device as force feedback, which results in the master device being forced upwards. This movement is then translated back to the slave site, and can be seen in the figure as the slightly delayed positional change.

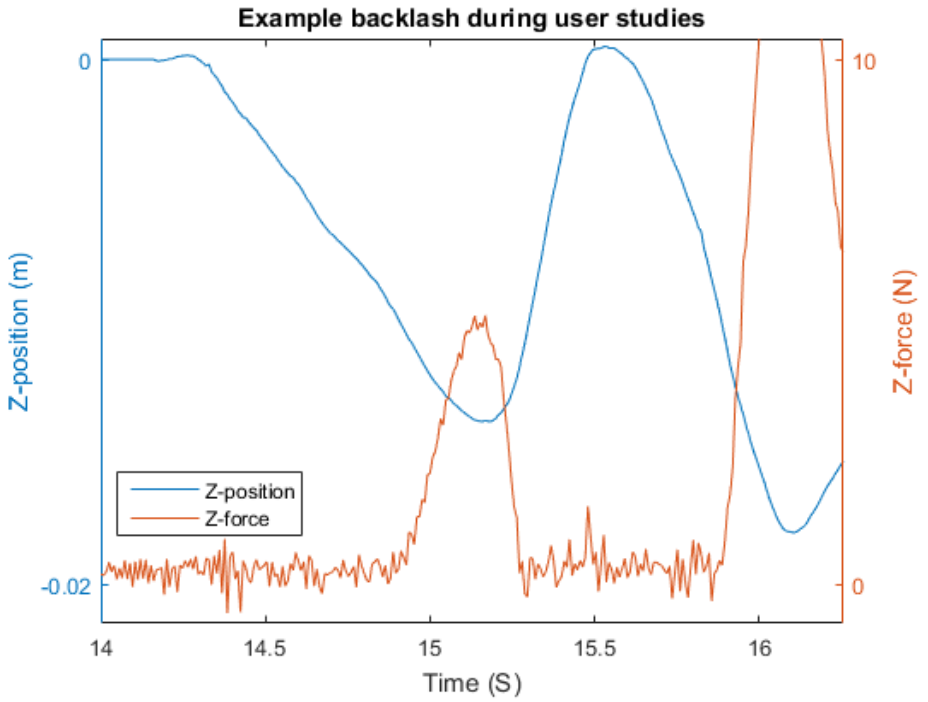

Figure 2.3: An example backlash response during the user studies in chapter 8

In [21], Heck et al. proposes a two-layer control architecture for a teleoperated system that incorporates force-reflecting while also being subject to time-delays. While the paper does not take into account a multi-DOF system, the results are promising. The two layers are called Performance Layer and Passivity Layer, or PeL and PaL, respectively. The PeL runs the normal controller algorithms, while the PaL keeps track of the force applied to the controller by both the operator and the environment. For the environment these forces can be seen as the force-feedback. By monitoring these forces the PaL introduces a damping gain to gradually reduce the control force of the PeL, thus removing the backlash, as well as unwanted chattering in the system. This is a good architecture, but means that you need a force-reading from both the master and the slave site of the system. For our system this would mean opening an extra channel in the Lawrence architecture seen in figure 3.4, which is currently closed.

Tension Cables For Minimally Invasive Surgery (MIS) stability is of great concern, as an unstable system within a patient could cause a lot of damage. A software implementation of force-reflecting requires a system fast enough to respond to changes, as well as a good algorithm implementation. Another way is to use a cable-driven haptic device, which is what is propsed by Qu et al. [22]. The reason they chose cables was to get a lightweight solution capable of avoiding backlash. This is a hardware level solution, and works by having tension cables apply the

force-feedback. These cables will increase in tension as the force builds up. This causes the controller to simply become stiffer, instead of using actuators which would physically push against the operators movements. In other words, cables causes force-feedback by not allowing downwards pressure, while actuators causes force-feedback by applying pressure in the opposite direction, which causes a backlash.

As it is possible to avoid backlash either through software, or simply with a more physical aproach to the problem by making use of preloaded bearings and pretensioned cables [23]. The latter solution sets hardware limitations on the system, and as such is less feasible for a system that should be usable for any haptic device with 6 DOF.

2.5 Hybrid Control

2.5.1 Conventional Force and Position Control

Position Control In robotics a normal control method for position and tracking tasks is the aptly named position control [24][25]. This control-loop uses the master devices' position as an input, and measures the difference between that, and the slave devices position to generate a new position command for the slave. This method works well for a system that does not rely on a precise amount of applied pressure to the work environment.

Force Control Another approach is by using a force feedback control, where the forces and torques at the end point of the manipulator is fed back to the controller. This then generates a velocity or position command based on the difference between the measured force, and the force setpoint value. In contrast to a position controller, this is a great way to control a robot manipulator when you have to worry about the actual forces being applied to the environment. With purely force control, however, tracking a preset path becomes an issue, as it will base its movement not on the position offset, but rather the force offset.

2.5.2 Hybrid Controller Schemes

Position-Force Hybrid Control A solution to these two problems is to quite intuitively combine these two control methods. This is a so called hybrid controller. Hsieh et al. puts it like this: "Force-position hybrid control methods aim to reduce the non-zero constraining forces involved in the pure position control method, and the position tracking errors involved in the pure force control method simultaneously" [26]. As such you get the best of both controllers, and end up with one method capable of both force-limitations, and position tracking.

Alternative Hybrid Control Methods There are other similar hybrid controllers, such as a velocity-force controller, which is described in Mathiassens' paper [27], or a force-posture controller proposed by Yao et al. [28]. In Yao's controller they use pose instead of position, which eliminates the need of calculating the inverse Jacobian. They manage this while also maintaining good control results. This could be useful in a real-time application, as calculating the inverse of a Jacobian matrix is a heavy task, which could impact the timing results.

A problem when designing a force-position controller is that the manipulators structure has to be very stiff. There must be a minimal amount of flex or naturally occurring oscillations when the manipulator moves in order for the force controller to be stable. In combination with this, the precision has to be very high. Meeting both of these requirements can be quite hard, as well as expensive, in commercially available manipulators. And as such it is something that has to be taken into consideration when designing a hybrid controlled system. The UR-5 robot used in this thesis upholds both of these requirements, being both rigid, and precise while keeping the price relatively low.

Medical Usage Fujie et al. [29] proposes a position-force controlled system in order to use a robotic manipulator to perform a laxity test on a human knee. A similar method has also been used to test the ligament forces in other human joints [30]. In a recent study, three such force-position controllers is proposed by Hsieh et al. [26]. They evaluate all three control methods for use in a robotic joint-testing system, and mentions the importance of development of more advanced and precise force-position controllers for use in clinical settings.

Control Parameters In a hybrid control system there are a multitude of parameters that needs to be tuned in order for the system to work optimally for the given task. While not a hybrid controlled system, Koizumi et al. [31] proposes pre-determined tuning values for a system depending on the type of examination to be performed. Another, more overall and robust method is presented by Hasan in [32], where neural networks and fuzzy control was used to create a one-step-ahead feedback control system. This allows for more adaptation when working with uncertain force and torque reflections from the surface. As such a system can either have pre-set control parameters, or employ an adaptive system capable of changing its tuning on the fly. Another example of an adaptive system with learning is presented by Jeon et al. in [33] where a system uses a feed-forward loop to continuously enhance the control performance as best possible every cycle of the control loop.

Continuum Manipulators Hybrid control is also used in so-called Continuum Robot Manipulators. These manipulators are often designed to operate in a constrained environment, where they have to rely on body com-

pliance to work around or with obstacles. In [34] Yip et al. proposes a model-less approach to a position-force controller for a continuum manipulator. Model-less control is an approach to control that allows the system to learn the manipulator Jacobian, and thus adapt to constraints in the environment in a safe manner. However such a model-less approach can end up in a poorly configured controller. Yip et al. presents a solution by using a hybrid controller, to control both the end effectors position and force, while still keeping the model-less controls minimalistic approach.

The hybrid position force control method, or a variation thereof, is a great control solution when it comes to human interaction. This is due to the fact that it allows for safety limitations to be implemented, while still using position control to perform specific tasks that a force controller would not allow for. The hybrid control scheme in general is also seen more and more as the industrial automation industry relies on contact forces, real time position and position control.

Chapter 3

Current Robot System

3.1 Previous Work

Previous work on this system includes the master thesis written by Jørgen Enger Fjellin [7]. His work involves the implementation of a bilateral master-slave system with haptic feedback using the UR5 robot [35] as the slave, and a Phantom Omni device [6] seen in *Figure 2.2* as the master controller. The UR5 robot is mounted with a combination of custom 3d-printed parts, aluminum and wood capable of holding the ultrasound probe. Along with this there is a six degree of freedom Gamma SI-65-5 force/torque sensor [36] connected, which makes the robot able to sense pressure applied to the end-piece, which in this case is the probe. This pressure is relayed back to the master haptic device and can be felt by the controller. The full implementation of the haptic control for our system is described in Fjellin's thesis [7].

Further work on the system has been done by Kim Mathiassen et al. [27]. In this paper the full system requirements for the ultrasound robotic system have been researched and discussed in detail based on earlier work in the field, such as the previously mentioned Hippocrate system [13].

3.2 System Overview

3.2.1 Hardware

An important feature of this thesis lies in the use of the UR5 robot. One of the key aspects of sing the UR5 robot is that it is commercially available, and it complies with point 5.10.5 of the standard EN ISO 13849-1:2008, which allows it to operate as a collaborative robot [35]. In other words, it is relatively safe to use around patients, and requires no additional safety guards between humans and the robot. The robot's safety mechanisms include stopping if the torque of any joint exceeds or deviates from the expected torque. A protective stop is also initiated if any of the joint velocities exceeds a preset value of 3.2 rad/s. All of these safety values are calculated and evaluated in the control hardware provided by Universal Robots. The robot also has three emergency stop buttons. Along with these safety features the robot is lightweight, and relatively low-cost, compared to other custom-made robots used for ultrasound examination, such as the Hippocrate system.

The force/torque exerted on the ultrasound probe is measured using a Gamma SI-65-5 from ATI Industrial Automation. There has recently been developed a new force/torque sensor that also includes a grip [37], which could work well for our system as it is made for use on the UR-robots. But for now the ATI Gamma is what will be used, as that is also the sensor analysed in the earlier parts of this project. Thus changing the force/torque sensor would require a re-adjustment and testing to ensure the system still meets the requirements.

The haptic device used in this system up until now has been the Phantom Omni [6]. This device offers 3 active DOF and 3 passive DOF and comes at a cheap price. While testing indicates that it works sufficiently well, Fjellin voices a concern that its maximum exertable force of $3.3N$ might be too low [7].

3.2.2 Software

The robot has three different levels of control, excluding the general control using the robots built in system and control-pad. One way is through a graphical user interface, which allows for simple tasks to be programmed. Another method is through scripts that can be sent to the robot and executed. The script however only accepts a limited type of external inputs, and cannot read the force and torque measurements from the ATI Gamma. The third way is the *C API*.

A software framework has been implemented which includes the robot's kinematics, control and safety features as well as interfaces to external sensors and data logging. The robot's kinematics and control uses the Armadillo C++ Linear Algebra Library for its implementation [38].

The main reason a custom software framework was developed by Kim Mathiassen was because the version of ROS at the time did not meet the required standards, or allow for real-time communication. In recent years ROS in general has been continously developed. Along with this an improved driver for the UR5 robot has also been developed [39]. This raises the question of whether or not the system should be moved and make use of ROS, instead of the custom framework. One big problem with using ROS is that it is still unable to operate a real-time system. For this thesis we will therefore use to the custom framework developed by Mathiassen.

The control system is running on a Linux computer with the help of the real-time extension Xenomai [40]. Xenomai creates a real-time system, which allows for the control process to execute before any other system processes. It should be noted that since the robot is implemented as a device, it has to use file operations to communicate. This means the control program has to switch from the real-time domain two times every cycle: Once when receiving, and once when sending data. According to an experiment in Mathiassen [27] this still allows the system to meet the real-time conditions.

User Interface The user interface is set up in Labview as a separate program. This is to separate it from the real-time processes, which allows for the control program to be more robust as the interface will not have to compete with the control system in priority. The control system and user interface connection are currently set up for use on a local computer. They

can however be changed to run on another computer for use in remote-control applications. The entire system overview can be seen in figure 3.1 below.

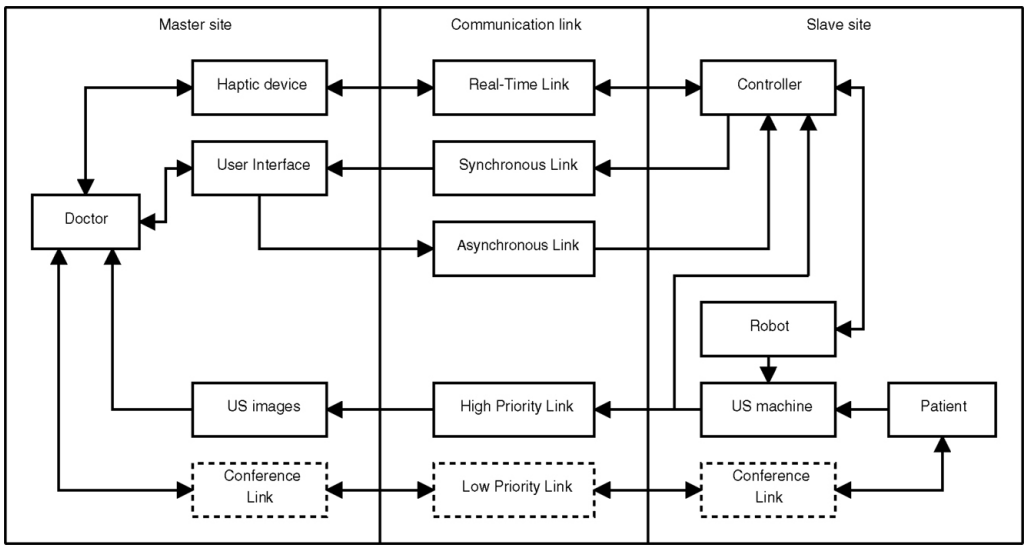

Figure 3.1: The current system setup [27].

3.3 Existing System Implementation

The inhouse extension of the framework has been developed at the Intervention Center. It incorporates a wrapper around the robot producers API, containing more intuitive and general calls to control the robot. The extensions allows for real-time control of the robot, which is critical in a clinical system. The wrapper is programmed into a daemon, which runs several real time threads. The threads perform tasks such as sending and receiving messages to and from the robot and reading data from the force-torque sensor. The daemon also allows external programs to send data to the robot through itself by using a real-time queue. The robot is updated at a frequency of $125Hz$ which is sufficient for a real-time system.

The robot can be commanded in several ways such as position, velocity or by force. A front-end in labview has been made in order to easily change which controller to use, and configure things such as setpoint parameters while the daemon is running.

For the force-torque sensor to work with the system the gravity bias of its own mass, as well as anything attached has to be calculated. This is done with a method described in [41]. In order to reduce the noise from the force-torque sensor an elliptic filter has been implemented.

3.3.1 Phantom Omni Device Communication and Control

The haptic device has been implemented using the OpenHaptics library from Geomagic (Formerly Sensable Technologies). This library is written in C, and split into two parts. HLAPI is wrapped around the HDAPI, and is used to simulate 3D environments. HDAPI is the part used for low-level communication and control of the haptic device, and as such is the only part that has been used in our system.

It was chosen not to make a dynamic model of neither the Haptic device (master) or the UR-5 robot (slave). Due to the small masses and velocities it was assumed that the inertia and coriolis effect could be neglected. As such the outcome was a control architecture that is independent of what device is plugged in at either end. A simplified software layout of the implementation is visualized in figure 3.2 with the block diagram for the calculations shown in figure 3.3. The code has been implemented in such a way that only cartesian coordinates, and forces are involved in the communication with the master and slave. Thus by changing the contents of a few methods and recompiling the code you can change the master and slave hardware.

The communication between the master and slave uses a two port network model. It is stated in [42] that it is possible to obtain transparency in a teleoperating system by implementing a forward flow Extended Lawrence Architecture. This architecture is shown in figure 3.4. This architecture sends velocity from the master, and force from the slave. As such it works well with teleoperation where force-feedback from the slave is a requirement. Along with this it is able to gain transparency with just two channels in the communications layer. This ensures a minimal amount of bandwith is necessary, and makes it ideal for communicating over a network, if that is to be implemented.

To remove the noise from the master device a low pass filter has been added with an original cutoff frequence of $55Hz$ and a period of three samples. The same filter, along with a 3 sample moving-average filter was added to the force readings to effectively remove the noise from the force-torque sensor. Both of these filters are described in more details in [7]. An in depth look at the transformations taking place between the masters and the robots movements can also be seen here. The system diagram for the haptic controller can be seen below in figure 3.3.

The upper part of figure 3.3 is the phantom omni master controller, which takes in a force measurement f_e from the force-torque sensor. This is then scaled down, before being sent to the haptic device. The haptic device delivers a new set of position commands T_m which are transformed into linear and angular velocities v_m and ω_m. The f_m is the haptic device's internal force controller. The two velocity commands are then sent to the

the robot, which is the slave part of the figure. Here the linear velocity is scaled up to match the robot, and the velocity commands are transformed into the robots frame, and sent to the robot as a velocity command $\dot{q}_cmd$.

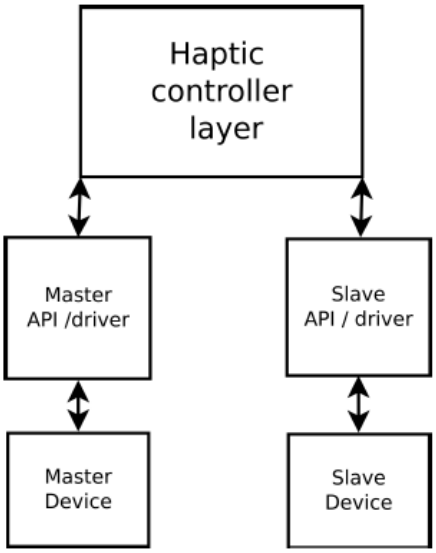

Figure 3.2: A simplified overview of the Haptic software implementation. [7]

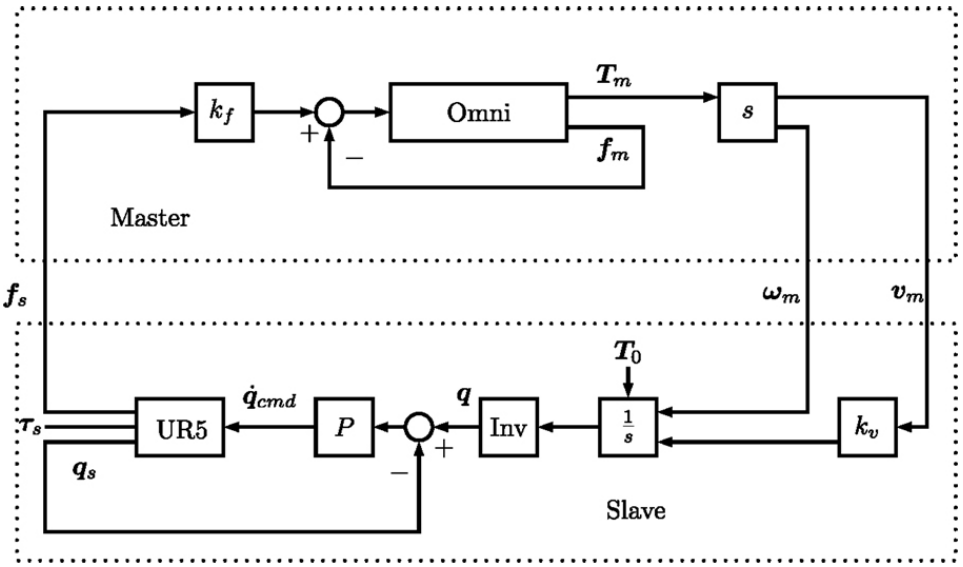

Figure 3.3: System diagram for the haptic controller [27]

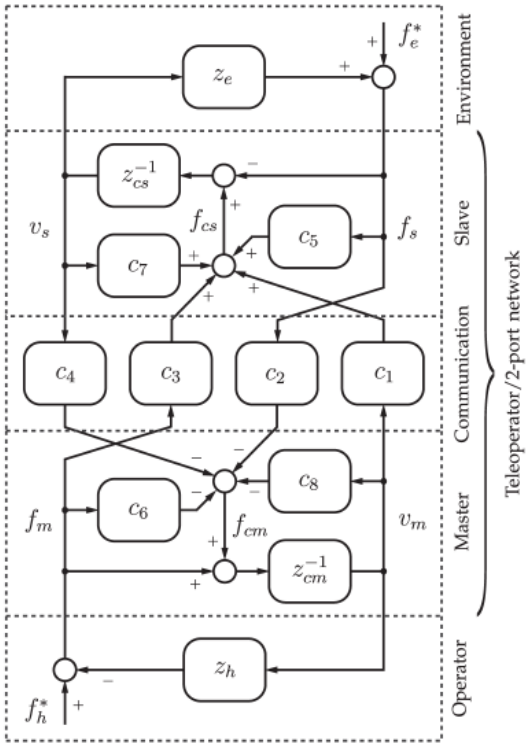

Figure 3.4: The Extended Lawrence Architecture. For a forward flow setup, gains c3 and c4 are set to zero. [27]

3.3.2 Stability

For systems using haptic force-feedback, stability is always an issue. A system can for the most part be made quite stable, if it is meant to work with either hard, or soft surfaces. The biggest problems arise when the system may encounter both types of surfaces. In the current implementation of the UR-5 haptic controller this is quite prevalent, and will pose an issue if the probe were to come in contact with bones while performing an examination. The current filtering of the system's signals is a low-pass filter, combined with a moving average filter to properly get rid of all the noise. This works very well when we work on soft tissue, and in the current ranges which are $8N - 20N$. These ranges are really low for harder tissues, or ultrasound examinations where you need to look at internal organs, which would require more pressure. As long as the amount of pressure is increased gradually the current system works, and we can simply set the force-limits higher. However, if you were to hit anything hard, for example bones, the filtering would not suffice. The sudden increase in pressure would require another type of filtering. For this paper we will focus on working with fairly soft tissue.

New low-pass filter Even so the low-pass filters cutoff frequency at $55Hz$ is too much for the material we will be working on. Our ultrasound phantom is described in section 6.1, and requires a change in the cutoff

frequency in order for the system to work optimally. The backlash is simply too great. The new cutoff frequency, $10Hz$, is found through testing and can naturally be altered depending on the material stiffness. Ideally more thorough testing should be performed on different kinds of material in order to find the best filter cutoff frequency for any given operation.

3.3.3 Velocity Limit

Originally the haptic controller was given two choices of internal limits for the velocity of the robot, based on the variation in force enacted on the patient. These are the Sigmoid Zero, and Sigmoid Low functions. The first one will lower the velocity of the robot towards zero as the amount of force applied to the patient increases. This is done by multiplying the velocity commands with the gain shown below in equation 3.1.

$$k = \frac{1}{1 + \exp^{(2*(abs(f)-4)}} \tag{3.1}$$

The Sigmoid Low will not set the velocity to zero, but instead go down to a predetermined minimum velocity as the force increases. Alongside these two functions there is a Static Low controller, which simply allows the robot to move at full speed, until it comes in contact with an object, at which point it will lower its speed to allow for more precise movements. These are described in more detail in [7], and for the rest of these experiments we will be using the Sigmoid Zero. Through testing done in [7] this was deemed the best option.

The Sigmoid Zero controller will be set up so the velocity goes towards zero as the force reaches a pre-determined value. This number can easily be changed to suit the radiologist's needs. The equation, and a sample response can be seen below in equation 3.1 and figure 3.5. For the response shown in figure 3.5, a maximum pressure of $8N$ was used. The result k from the equation is the velocity gain of the robot.

This equation can be tuned to give the proper gain for the examination at hand, whether a minimal amount of force is to be used, or a lot. For use on our phantom, described in section 6.1, the Sigmoid controller will be tuned in a way which makes the velocity reach zero as the force reaches the optimal value for a clear ultrasound image. This of course requires that we already know the force necessary so that we can preload the equation with the force data. In a clinical environment, setting up pre-set values for this controller can help the radiologist perform standard ultrasound examinations, while also being able to tune the values if more force is necessary. Being able to change this equation on the fly could also prove useful, in case a need for more force arises during an examination. For now it is implemented in such a way that the values must be locked in before the examination starts. The best way to make use of this velocity limit is

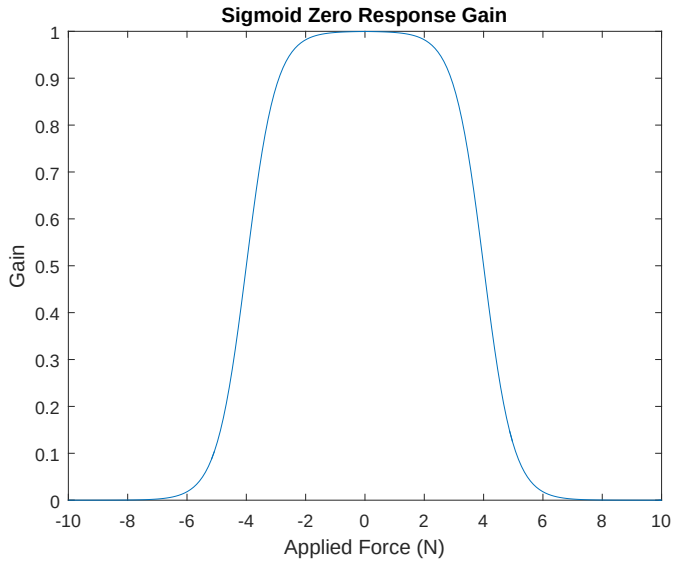

Figure 3.5: The response of the Sigmoid Zero controller. The X-axis is the measured force, and the Y-axis is the computed gain for the robots velocity.

thus to set it slightly above what you will need for any given examinations, to give the radiologist some leeway while still maintaining patient safety.

There are three more velocity controllers available, being the Transparent, static low and a controller with no force feedback. Only the second of these three alters the velocity, but does not do so gradually, and was deemed the worst of the three controller algorithms. The remaining two can simply be used for testing purposes, but serve no real purpose in the finished system. As such these three will be overlooked.

3.3.4 Compliance Force Control

The force controller that will be used for the hybrid controlling scheme developed in this thesis will be a compliance force controller. This controller has been implemented by Mathiassen, and uses the control law from [43]. A dampening term is included in the control law, to filter out the vibration in the robot. This is explained more in depth in Mathiassen's paper [27]. The final equation, resulting in joint velocities, is shown below in equation 3.2. The resulting $\dot{q}_o$ is the joint velocity command being sent to the robot. The force setpoint is set by the user, and f_e is calculated by taking the force setpoint minus the measured force. K is the compliance matrix, which is a diagonal matrix containing the gain for all 6 dof. And K_I is the dampening term, which can be seen as integration term, smoothing out the robots vibration noise.

$$\dot{q}_o[k] = J^{-1}(Kf_e[k] + K_I v_d[k-1]) \tag{3.2}$$

Parameter Tuning A couple of different parameters were tested for the compliance force control, but in the end the results from Mathiassen's paper proved to work best. The experiments and a more in-depth look at

different tuning parameters can be seen in his paper [27]. The parameters used is $K = 0.05$ and $K_I = 0.8$. The results during a step response while in contact with the phantom is shown in section 7.2.2.

The compliance matrix used in this force controller is not to be confused with the similarly called compliance matrix in the hybrid controlling scheme. The force controllers matrix K simply allows for a different gain for every DOF, while the hybrid compliance matrix S decides which DOF should be controlled by position or force. The latter is explained in Chapter 5

Chapter 4

Improvements to the Existing System

4.1 Maximum Force Limit

There is another important safety measure that must be implemented. While the previous algorithms limit the velocity of the robot, they do not take into account any errors in the haptic device. Except for the upper hard limits set within the robot software, there is no proper force limit based on the velocity from the haptic. Any error that happens in the controller will not stop the robot from moving, as it simply follows the master controller's movement.

The Phantom Omni has a built in limit, which keeps it from giving out more force-feedback than its actuators can take. The force-feedback will disappear if the system is overloaded. This is easily achieved, even by mistake, as the controller is quite weak [6]. When the force-feedback disappears, the controller will feel transparent. This causes a sudden jolt in the master's movement. In turn, this causes huge velocity readings to be sent to the robot. Even with the velocity limiting algorithms, such as the Sigmoid Zero, the robot will still move when this happens. Some of the movement often comes from the fact that the force has not yet reached a point where velocity is tuned fully down to zero through the Sigmoid equation gain. Most of the movement, however, comes in the form of rotation around the point of contact. The rotations does not in theory change the x, y or z-velocity of the end effector, and as such they are allowed. But since the probe is not a symmetrical sphere a rotation will still, in a lot of cases, increase the downwards pressure since the rotation itself forces the ultrasound probe further down. Usually the force is already quite big, so any small movements such as this will cause an unwanted, and big spike in pressure towards the patient.

The problem could be limited by using a more powerful controller. But the system should be safe to use for any haptic controllers. Therefore an additional safety feature has been implemented. It is an extension of the Sigmoid Zero algorithm.

There is, as mentioned, already an over-riding force-limit on the slave side, which is set to $100N$ [27]. This limit is based on the research done in [44], which states that the necessary force for certain examinations can reach this value. But this limit is too high for some kinds of examinations, which can range from as low as $4 - 7N$ [1]. For example in carotid artery examinations. As such we will leave the upper limit as is, and instead implement an additional limit which can be changed, based on what type of ultrasound examination is taking place. Another reason why we do not use this upper limit is that it is set up in a way that makes the robot lock up. This makes it serve well as an absolute safety feature, but makes it unreliable for an examination since you would have to continuously unlock the robots joints if the limit is reached.

By adding an extra part in the algorithm we are able to set the velocity to absolute zero on the slave site if the robot exerts too much force in a given direction, without locking up the robot. This force-limit is to be set at a higher pressure than the Sigmoid Zero "soft" limit. This way, the Sigmoid controller will be the actual working controller, while this limit is a safety feature, should the haptic device fail.

The way this is done is by continuously checking the current force-reading against a pre-set maximum. If the forces exceed the maximum, the velocity in that direction is set to zero. In our case the direction will always be the z-direction of the end effector. If the applied force goes below the maximum again, or you attempt to move away from the point of contact, the velocity-lock is released and you are allowed to move. The directional check works by checking the force and velocity on the same axis. If $fv > 0$ we are moving away from the target, and in the same way if $fv < 0$ we are moving towards the target.

$$v_z = \begin{cases} 0 & \text{if } f_z > limit \text{ and} fv < 0 \\ k * v_z & \text{if } fv_z > 0 \end{cases} \tag{4.1}$$

The variable k is the gain from the Sigmoid Zero, as seen in equation 3.1. The rotation will also be slowed down at this point, but not stopped entirely. That is because its hard to predetermine the rotation that might happen in a scenario where the haptic fails. Because of this, if we were to stop the rotation, we could get stuck and not be allowed to move at all. Unfortunately this means that a failure in the haptic device can still cause an increased pressure, but now it will only be due to rotation.

In figure 4.1 and figure 4.2 we see the response when the haptic fails. The values measured are the z-position of the master, and the z-directional force of the slave. Figure 4.1 shows the results without a force-limit. At roughly 0.8 seconds the haptic device fails. This causes the sudden downwards movement of the master, which results in the increased pressure at the slave site, as the slave robot will also move downwards. Figure 4.2 shows a similar haptic failure, this time with the force-limit implemented. At 0.1 seconds the haptic fails, causing a sudden downwards movement, but since the slaves downwards movements are limited, the force does not increase the same way as in figure 4.1.

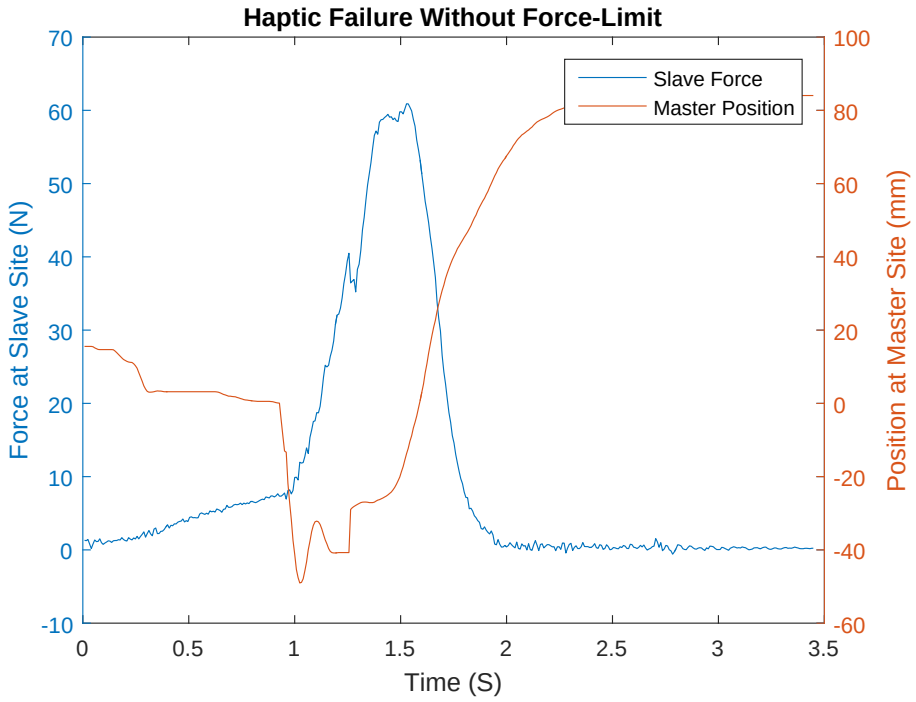

Figure 4.1: The resulting master movement and slave force when the haptic device fails, before implementing a force-limit

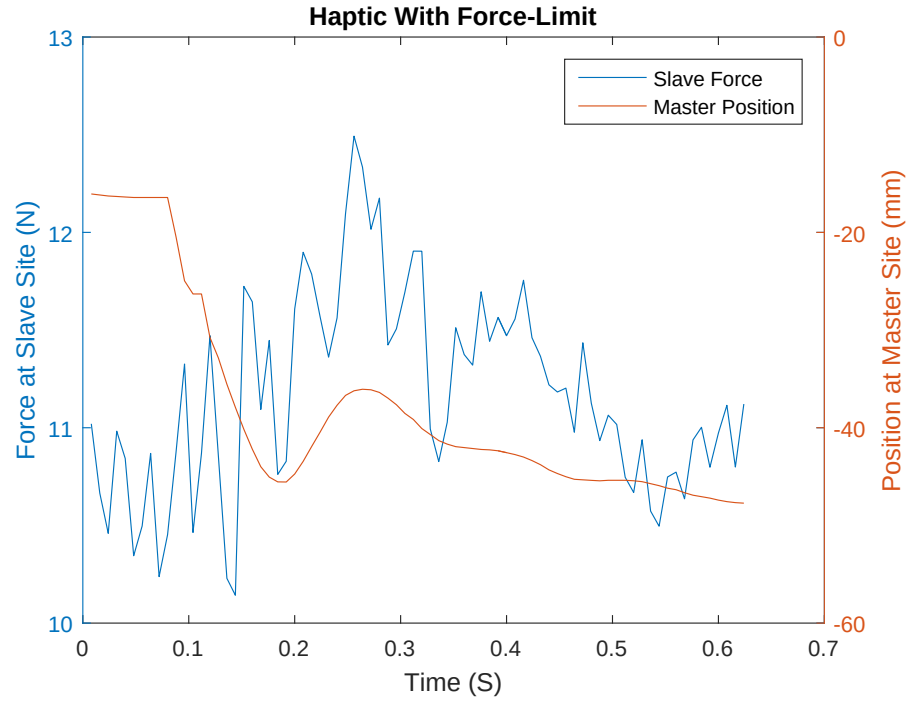

Figure 4.2: The resulting master movement and slave force when the haptic device fails, with a force-limit

4.2 Force Reflecting

As we are making a system for use with multiple kinds of haptic devices, we can not avoid a backlash in the controller by using specific hardware, such as the one described in [23]. Instead a software solution have to be implemented. In [21] a two-layer architecture is presented to make a force reflecting system. This system even takes into account time-delays, which will become a bigger concern once our system is set up to be used remotely. The paper, however, only proposes a single DOF solution. And since our system should work for 6 DOF, a simpler solution has been put in place.

The force being sent back to the controller is continuously dampened when in contact with a material. The way this is done is by adding a dampening factor k, and multiply it by the force. For simplicity this dampening factor is a value between $0 < k < 10000$, which increases by 5 for every run of the loop as long as pressure is applied to the force-torque sensor. The force is then calculated as shown in equation 4.2. The resulting value of this equation can easily be tuned to fit either more scientific requirements, or personal preferences.

$$F_{master} = \frac{F_{measured}}{k_{max}} * k \tag{4.2}$$

The reason it is done like this is simply because it allows us to scale the force up for every run of the control loop with a simple command. It should be noted that this scaling only occurs in the end effector's z-direction, as that is the direction of operation in most cases.

While the probe is moving in free-air, the force feedback is essentially zero, and this dampening does not affect the system. Once the probe comes in contact with an object, the low pass filter will remove a lot of the initial backlash. This scale factor will help by making it so that the force feedback will be slowly scaled up to full, which further dissipates any backlash. Once the damping factor has been fully saturated it stays that way until the measured force drops below a given threshold of $3N$.

This limit of $3N$ is set based on the usual range of necessary force during an examination, which is stated to be from $4N$ and up [1]. After the initial contact is made you would thus have full force-feedback throughout the examination. But in cases where you have to move the probe away from the patient to readjust the position, you would reset the calculations, and the system would be prepared for a new "initial contact" phase.

Chapter 5

New Hybrid Controller

The robot works by using either a so called *external controller*, which makes use of an external controller program running the Phantom Omni kinematics and control, or *internal controllers*. The *internal controllers* refer to the controllers which do not require any data from an outside program. The *external controller*, in this case the haptic controller, receives and sends data to an external program. The new hybrid controller will combine the haptic controlling scheme with a force-controller.

5.1 Current Hybrid Velocity-Force Controller

As has been discussed, we already have a working external haptic controller. There has also been implemented an internal Hybrid Force/velocity controller, which is capable of choosing which degrees of freedom should be controlled by force, and which should be controlled by velocity. This force-velocity hybrid controller is described in Mathiassen's paper [27]. The controller is set up to allow for a constant pressure in one dimension, while still allowing for free movement in other dimensions using velocity control. The control loop for this is shown in figure 5.1.

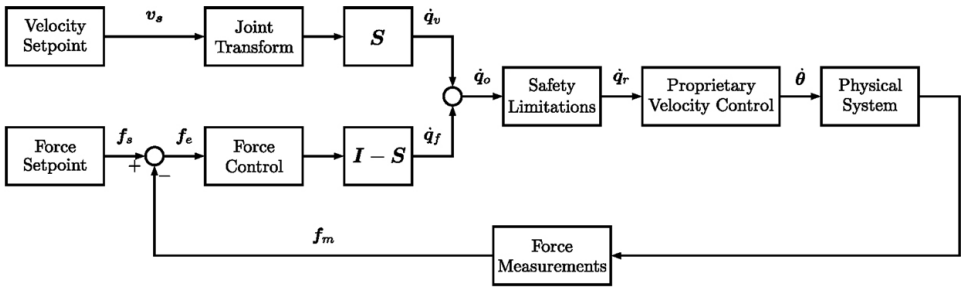

Figure 5.1: The control loop for Mathiassen's Hybrid Force Controller [27]

This controller is unfortunately not possible to integrate with the haptic controller as is. The Phantom Omni Haptic Device is not capable of delivering rotational velocity, and as such we can not simply feed velocity commands from the external haptic controller into this hybrid controller. Another issue that would arise with a velocity controller, when using a master haptic device, is oscillations. This is due to the delay present in such a system. Therefore we keep the positional control scheme for the haptic device, and instead make a new hybrid *position-force* controller.

5.2 New Hybrid Position-Force Controller

Figure 5.2 shows the proposed force-position controller. The force controller part, as well as *Pz* in the position controller, will only be activated when a button is pushed. The position controller is explained more in depth in Fjellin's thesis[7] and the force controller in Mathiassen's paper [27].

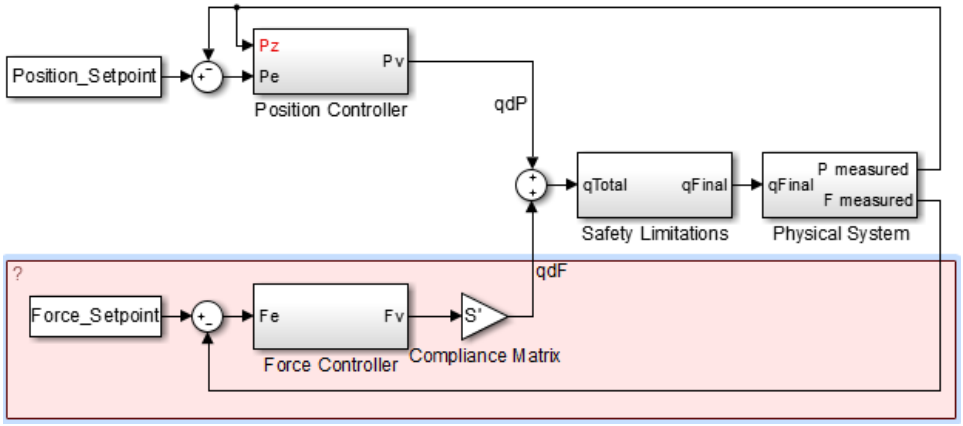

Figure 5.2: The proposed simplified hybrid position-force control loop

The upper part of the loop in figure 5.2 is the haptic position controller, also shown in figure 3.3, while the bottom part is the slave's internal compliance force controller from section 3.3.4. The position controller has been changed to either control all degrees of freedom, or everything except for the position in z-direction. It can, however, be modified to include the compliance matrix. This would allow us to have one unified control over which directions of freedom should be controlled by which controller. The transformation to joint velocities is not shown in the figure. Only the resulting qdP and qdF ($\dot{q}P$ and $\dot{q}F$) is noted down.

The compliance matrix S, is a $6x6$ matrix with zeros or ones along its diagonal, shown in equation 5.1. The first three diagonal values define x, y and z directional velocities, while the last three define the rotational jaw, pitch and roll velocities. Its values can be set in the labview front panel, shown in figure 5.3. The upper left display shows the current values along the S matrix diagonal, while the upper right display is where you input new values.

$$\begin{bmatrix} v_x & 0 & & \dots & & 0 \\ 0 & v_y & 0 & & & \\ & 0 & v_z & 0 & & \vdots \\ \vdots & & 0 & v_\alpha & 0 & \\ & & & 0 & v_\beta & 0 \\ 0 & & \dots & & 0 & v_\gamma \end{bmatrix} \tag{5.1}$$

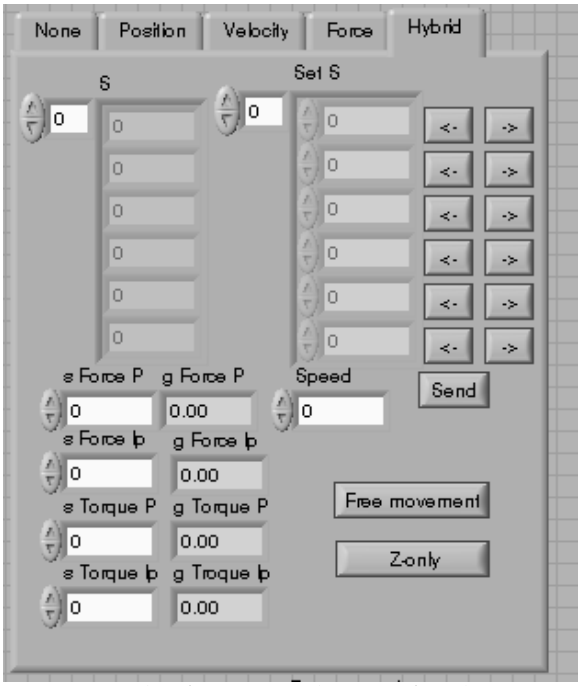

Figure 5.3: The front panel input for the S matrix

It is used by the force controller to determine which degrees of freedom it should have control over. When the velocity commands from the force controller is transformed into joint velocities, the inverse Jacobian is multiplied with the compliance matrix, as shown in equation 5.2. F_v is calculated as shown in equation 3.2. This zeros out any velocity commands that would cause movement in any direction, other than what is defined as 0 along the diagonal of the compliance matrix. The reason for it being 0, instead of 1, is because we use S' for the force controller. Originally S was meant to be used in the position controller.

$$\mathbf{qdF = S' J^{-1} Fv} \tag{5.2}$$

When the button is pushed, the setpoint of the position controller is taken from the robot's measured z-position, instead of the haptic devices z-position output. This way the position controller will not attempt to make any changes in this direction, as the position error will always be calculated as zero. By doing this the position controllers velocity output will not fight against the velocity output in z-direction coming from the force controller.

When the button is pushed again, the force controller output is set back to zero, and the position controller regains full control of all six degrees of freedom. When first initiated, the hybrid controller runs a test. This test checks the starting output/position of the button. It is important that the hybrid controller starts out with the force controller disengaged, so the robot does not move unexpectedly during the start of a procedure.

$$ButtonPressed = \begin{cases} 0 & \text{if } initPos == currentPos \\ 1 & \text{if } initPos \text{ != } currentpos \end{cases} \tag{5.3}$$

5.3 Controller Change Button

For the operator it is important that the change between position or hybrid control is as seamless as possible. This is in case the position of the probe, or the applied pressure, needs to be adjusted. In some cases it is better to move the probe away from the patient and reposition it completely, instead of dragging it along the patient. For small adjustments however, you may want to keep the constant downwards pressure in order to maintain a clear ultrasound image.

For safety reasons there are buttons connected to the robot that the radiologist can press in order to lock the robot's movement. That means both of the radiologists hands are busy, as one hand would be on the controller, and another on a safety button. A way to solve this is to use a pedal that can be operated with the foot. An example of a pedal setup can be seen in the AESOP system [45], and should be a good solution.

This pedal will be connected to the UR-5 robot in the same way as the custom made emergency stop buttons. The emergency button is shown in figure 5.4a and the digital input port in figure 5.4. It will be read in through the robot's API as a digital input, giving either a value of 1 or 0. The pedal uses a spring loaded on/off switch. This is so that the radiologist does not have to maintain pressure on the pedal. The pedal is shown in figure 5.5.

(a) Safety button (right) next to the haptic device

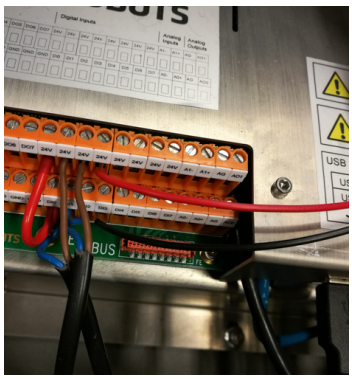

(b) The digital input ports on the UR-5

Figure 5.4: Safety button and input channels

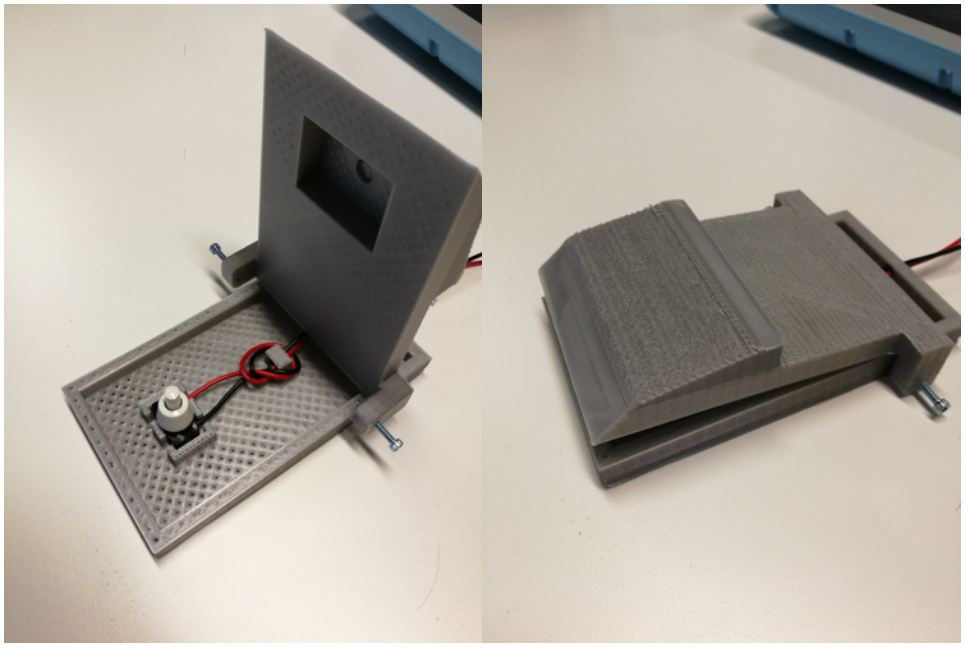

(a) The interior of the pedal (b) The pedal when in use

Figure 5.5: The controller change pedal

How the haptic controller should behave once the pedal is pressed is a factor that has to be tested. When attempting to find the right pressure, the radiologist naturally applies pressure with the haptic device. When the pedal is pressed down the first time, the force controller takes over the downwards pressure. At this point the original thought was for the force-feedback to be reset, with the newly found pressure as the zero position. This would allow the user to more properly gauge any additional pressure changes. When the pressure is found, the haptic is likely already fully saturated which would mean any additional pressure would not be felt on the master site unless we do this. Resetting the force did however prove to make the system quite unstable, and very hard to use.

This problem stems from the fact that the system is tuned to work with a gradually increasing amount of force with zero as its origin. By setting, for example $10N$, as the new zero-position we run into trouble with how the system is tuned. As the applied pressure rises, naturally the stiffness of the material rises as well. Thus any small movement in position, when higher force measurements are present, will cause a bigger change in the applied force than the system expects. This makes the system unstable, as all the velocity limiting algorithms, as well as the force feedback, simply are not tuned to handle the rapid changes in force, resulting from such minuscule movements of the end effector.

A solution that works is to simply scale down the force-feedback for the probes x and y directional movements, and remove it altogether for the z-

direction, which is its downwards pressure. The reason the z-directional force feedback is removed entirely is because the applied force in this direction is handled by the force controller at this point. As such there is no point in the operator maintaining this pressure on the master site when moving the probe around.

Chapter 6

System Experiments

6.1 Ultrasound Phantom

To start the testing procedure, and build upon the master Thesis of Fjellin [7], we have to make a test phantom. The material will be harder than a normal human body, but the controller can be tuned to work with either hard or soft material. The more important part is that the material attenuate the ultrasound beams so the things hidden in the phantom will show up on the ultrasound image.

6.1.1 Human-Like Test Tissue

The recommended attenuation coefficient slopes when making a phantom ultrasound material should range from $0.3 - 0.7 dBcm^{-}1MHz^{-1}$ [46]. There should also be a low backscatter level, to avoid noise in the image. For many years water-based rigid gels with microscopic graphite particles have been used. There are different materials available, such as the one reported in [46]. This material is made using evaporated milk, which is available in most grocery stores. Thus this material is both easy to make, and also upholds both the standards for ultrasonic beam attenuation, and backscatter levels. But getting a hold of the soluble agent to keep the bacterial levels down proved to be hard. The paper suggested *thimerosal* (product no. T8784, Sigma Chemical Company, St. Louis, MO, USA). As such we will stick to the more normal water based gel with graphite particles.

The mixture consists of 95% water, 4% graphite and 0.75% agarose. This makes for a ideal material for ultrasound examinations, as it meets the requirements mentioned earlier. It is relatively stiff, and the spring constant will give us an idea of how to best tune our system to work for this phantom. One issue with this phantom is that it will produce mold after a while. So it has to stay refrigerated when not in use, and can only be used for so long before it dries up. A way to counteract this is to add an extra chemical, but since said chemical is slightly poisonous we choose to leave it out. The completed phantom is shown in figure 6.5a.

6.1.2 Spring Constant

We can estimate the hardness of the phantom by using the definition for spring constant seen in equation 6.1.

$$F = k\Delta p, \qquad k = \frac{F}{\Delta p} \tag{6.1}$$

By using the haptic controller we can have the robot touch the phantom, and then move it into the phantom gradually. By measuring the change in position and force we can estimate the spring constant of the phantom. Since the phantom is placed in the XY plane of the robots base, we only concern ourself with the Z-domain of the robots base frame. Below in

figure 6.1a the measured force of the test can be seen, and figure 6.1b shows the position of the probe. In the position graph it can be seen that initial contact with the phantom is made at roughly sample 1100. The downwards movement at the start of the measurements comes from the fact that the probe starts in free-air. A small backlash occurs upon contanct before a stable contact is made. As the figure 6.1a shows, the force increases faster as the probe presses further into the phantom.

We are not interested in the free air movement of the probe, and as such we will estimate the spring constant based on the readings from sample $1700 - 3000$. For ΔP we can estimate the point of contact to be at roughly $0.156m$, seen in figure 6.1b at sample 800. This allows us to set a proper starting position. Figure 6.2 shows the calculated k-value for the given subset. By taking the mean value of this subset we get an estimated value $k = 1234N/m$.

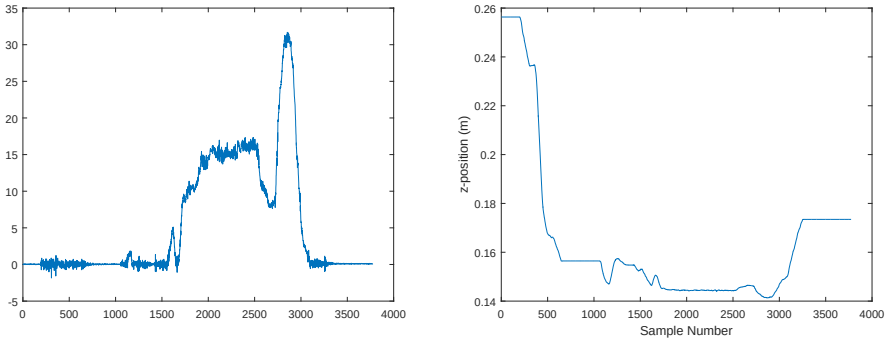

(a) The force of the slave, measured in the z-domain of the slave's base

(b) Position of the slave measured in the Z-domain of the slave's base

Figure 6.1: Force and position of the slave in the z-domain

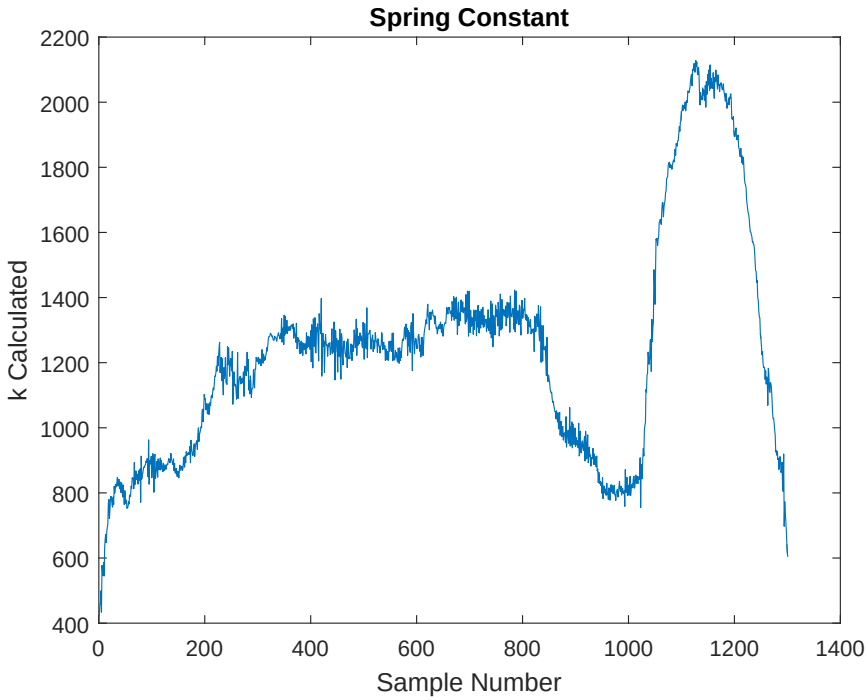

Figure 6.2: The calculated spring constant K over the sample subset 1700-3000 from figure 6.1b and figure 6.1a

This is a rough estimation of the spring constant, but it goes to show that we are working on a rather stiff object. In earlier testing of the haptic controll system the phantom that was used ruptured at roughly $15N$ of pressure [7]. Thus we are capable of working with more than double the amount of pressure, compared to earlier testing. This may allow for more rigorous testing of the system. It must be noted that the phantom was not pressed to its limit, and therefore the spring constant is not an exact calculation off the actual value.

6.1.3 Objects in the Phantom

A pattern of fishing lines has been spanned at varying depths within the phantom. In the 2D image created by the ultrasound examinations these lines will show up as dots, which should be clearly visible. There are two sets of lines, perpendicular to each other. This is to promote rotation of the probe during a test-procedure. A 2D view of the phantom, as seen from either side is shown below in figure 6.3 and 6.4.

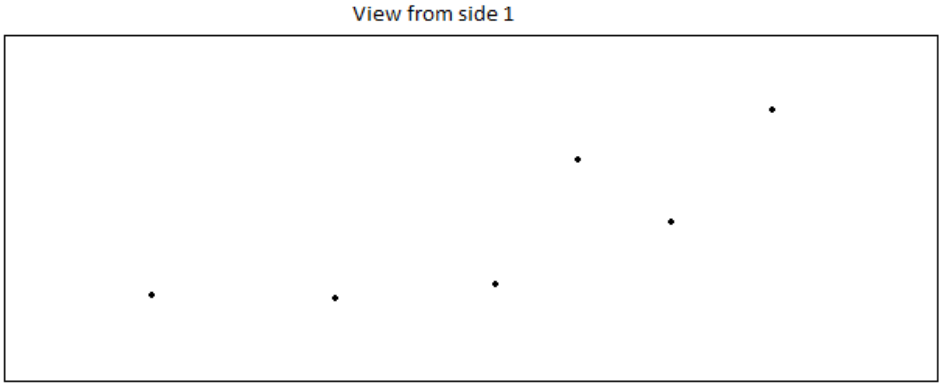

Figure 6.3: Side 1 of the ultrasound phantom. Dots shown are the lines seen from the front, perpendicular to those in figure 6.4

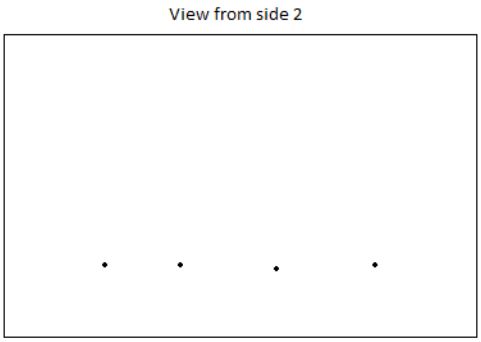

Figure 6.4: Side 2 of the ultrasound phantom, dots shown are the lines seen from the front, perpendicular to those in figure 6.3

In a perfect ultrasound examination all of these dots should be extinguishable by the radiologist, if the probe is rotated in such a way that the fishing lines point straight into the ultrasound field. Because we have two sets of lines perpendicular to each other the user will have to rotate the probe to get a clear view of all lines.

6.1.4 The Finished Phantom

In figure 6.5a the finished product can be seen. It is encased in a plastic container. While the plastic makes the ultrasound bounce back to the probe, creating unwanted reflections in the ultrasound image, it is still usable. Everything down to roughly 5 *cm* is clearly distinguishable. An example image is shown in figure 6.5b. The people testing the system will simply be told to overlook everything below that depth.

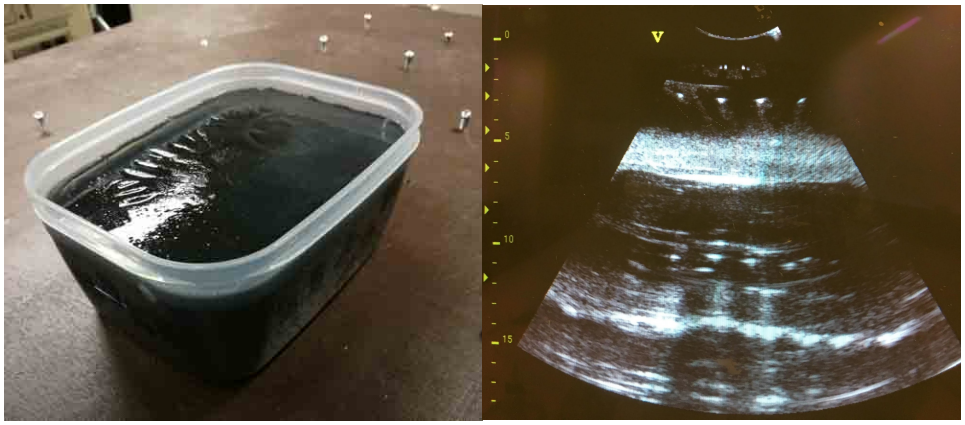

(a) The finished ultrasound phantom (b) An ultrasound image of the phantom

Figure 6.5: [
The phantom (a) and an example ultrasound image of it (b)]The phantom (a) and an example ultrasound image of it (b). The four points from figure 6.4 are seen as the four points near the top of (b)

6.2 Real-Time Performance

There are two reasons why we test the real-time performance. One is to ensure that the domain switches do not affect the system, as these could slow the system down. The other reason is to ensure the system is simply fast enough to be called a real-time system.

Because this system is built upon an already existing system some of the tests that were performed before will be re-run, in order to confirm that the new controller still acts within the required parameters. The most important one is the real-time performance of the new hybrid controller. It is necessary that it can run within the timing of the overlying system's loop, which is the one that defines the system's timing.

There are two timing variables being logged. One is the *control-cycle timing*, and the other is the *control-loop timing*. The cycle time is how long one entire cycle of the control program takes, while the control loop time is simply the time the calculations of the chosen controller takes to compute. In our case the control-loop time would be the execution time of the hybrid controller calculations, while the control cycle time would be the overlying system's time, including sending and receiving data. As long as the control-loop time is shorter than the cycle time it does not affect the system's real-time performance. But we still want to stay as low as possible so the timing variations of the loop time are still well within the cycle time.

6.2.1 Control Cycle Timing

The system runs at 125 Hz, which means that it should have a period of 8 ms. This was proven to be true in Mathiassen's paper [27]. Since all the changes to the system are done in the controller algorithm, all these changes will be reflected in the control-loop time. As such, the control-cycle time should not have changed.

6.2.2 Control Loop Timing

Without Hybrid Control The force control part of the hybrid controller will only be initiated once a button is pressed, as described in section 5.3. Because of this it is possible to test the timing of the controller without the force controller calculations being run, making it the same conventional haptic position controller developed in [7]. We do this because some changes have been made to Fjellin's original haptic controller before we built it into the hybrid controller. Thus we want to make sure it still runs as fast as it used to.

With Hybrid Control Activating the hybrid control scheme should make the control-loop timing slightly worse, as there are more calculations done. The inverse jacobian calculations necessary to get the joint velocities, shown in equation 3.2, are especially taxing. This should show up as an increase in the control-loop timing.

6.3 General Performance

6.3.1 Forward Flow Haptic Control

As mentioned, some changes have been made since the forward flow haptic controller was tested in [27]. For the free air movement the tests will be run both with and without the compliance force controller activated. The first test is done to compare the new edited haptic controller against the old one reported in Mathiassen's paper. The second test allows us to see how the extra timing delay of the compliance force controller impacts the position controller's bandwidth.

The transparency will be calculated with the compliance force control disengaged. This is because the compliance force control does not send any data back to the master. And as such there is no transparency to speak of. The compliance force controller itself will be tested afterwards, as a separate controller.

Free-Air Movement In the first test the master will be rapidly moved from one point to another, to simulate a step-like input in the position domain. By using the master's position as input, and the slave's position as output we will find the transfer function, and the bandwidth of the position

control of the slave. The first test without hybrid control will give us the bandwidth of the updated haptic controller, while the second test with the hybrid control activated will give us the bandwidth when the hybrid controller is engaged.

In Contact with the Phantom In the second experiment we move the probe up and down while in contact with the phantom. This allows us to estimate the transfer function and the bandwidth of the force control of the master. This gives us the transfer function of the data being sent from the robot and back to the haptic, which is necessary to calculate the transparency of the system. As mentioned this will be done without hybrid control.

It is important not to confuse the haptic force control, which is a force control for the master device, with the compliance force control, which is the controller for the slave device. The first one is the controller that takes the force from the robot, and generates force feedback for the operator. The second one is the hybrid compliance force control, seen as the upper part of figure 3.3. This controller works on the slave side, but does not send any data back to the operator, and therefore plays no part in the transparency of the system. Once a setpoint force has been given to the force part of the hybrid controller it will run separately from the haptic controller.

6.3.2 Compliance Force Control

For this force control test we will set the starting pressure at $5N$, and then increase it to $10N$ without using the haptic controller. In a normal operating scenario the setpoint for the compliance force control will come directly from the measured force of the force-torque sensor. But in order to create a step-like input in this experiment we instead use the labview front panel to set these setpoint forces directly, and accurately. This allows us to test the force controller part of the hybrid controller, and see how well it functions both in pressure step changes, and while maintaining pressure.

6.3.3 Transparency

With the two tests from 6.3.1 completed we have all the data we need in order to find the transparency of the system. This gives us an indication of how well the system works as a haptic control scheme. In [47] transparency is defined as master impedance divided by slave impedance. The mechanical definition of impedance is $Z = \frac{F(s)}{V(s)}$.

Using Zandsteeg's formula we have $T_p(s) = \frac{Z_{master}(s)}{Z_{slave}(s)}$, and we know $V(s) = sP(s)$. The force and position transfer functions then gives us the transparency shown in equation 6.2.

$$H_f(s) = \frac{F_{master}(s)}{F_{slave}(s)} \; H_p(s) = \frac{P_{slave}(s)}{P_{master}(s)}$$

$$T_p(s) = \frac{F_{master}(s)}{sP_{master}(s)} \frac{sP_{slave}(s)}{F_{slave}(s)} = H_f(s)H_p(s) \tag{6.2}$$

In other words we can get the transparency of the system by multiplying the two transfer functions we estimated earlier.

Chapter 7

System Results

In this chapter, any reference to the haptic controller simply means we are running the hybrid controller without the compliance force controller engaged. This makes the hybrid controller into a simple forward flow haptic controller. The data gathered from this control method can be compared to the old test results in Fjellin's paper [7].

7.1 Real-Time Performance

The results for the control cycle can be seen in table 7.1. As mentioned in section 6.2.1 it has not changed and remains at roughly 8ms.

Avarage Period (ms)	SD (ms)
8.020	0.021

Table 7.1: Control cycle timing results. *SD = Standard deviation*

Table 7.2 shows the timing result from the control loop both with and without the compliance force control engaged. The loop time is well within the cycle time for both. This can also be seen in figure 7.1. The loop timing roughly doubles with the compliance force controller activated.

	Avarage Period (ms)	SD (ms)
Forward flow haptic control	0.282	0.139
Hybrid controller	0.509	0.191

Table 7.2: Control loop timing results. *SD = Standard deviation*

Figure 7.1 shows that the compliance force controller is activated roughly three seconds into the run. The loop timing increases to about double of what it was when running only the haptic controller. The spikes that can be seen throughout the the run is a result of the data-logging happening inside a real-time thread. Logging the data is a file-handling task which brings the system out of the real-time domain. This causes disturbances which show up on the timing results. These periodic spikes disappear when we stop logging the data to a file. Thus they cause no issues in the system when run normally.

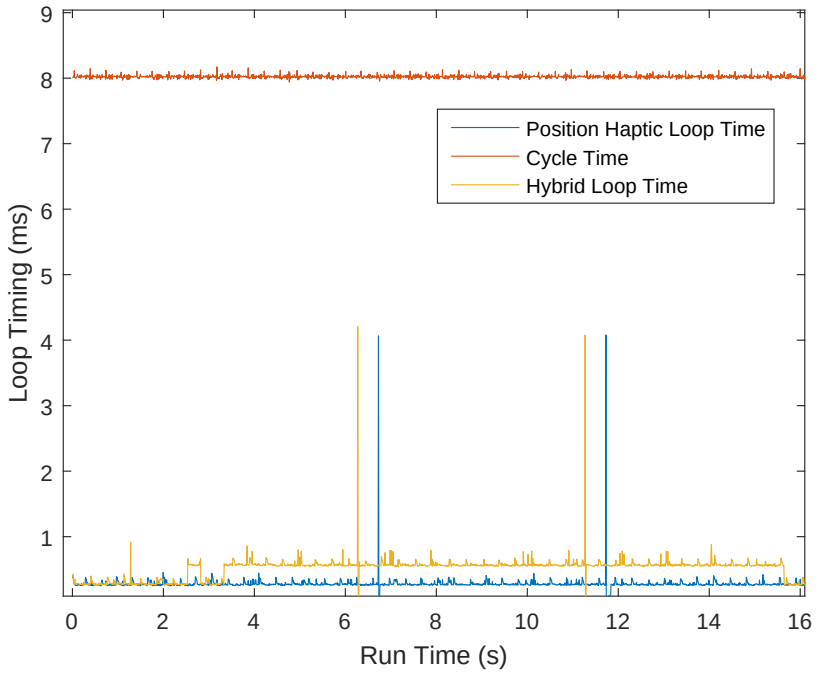

Figure 7.1: The result from timing the position haptic controller, and the hybrid controller loops

7.2 General Performance

7.2.1 Forward Flow Haptic Control

In figure 7.2 the step response of the master according to the slave movement is shown. The positions are transformed into the same frame of reference in order to be properly compared. There is a slight overshoot in the slave position, but this overshoot is a scaling constant. Since we are not using any pre-set positions, but rather get our slave position continuously from the master device, a deviation like this does not pose a problem.

The system is estimated as a Single Input Single Output (SISO), and the step is performed in the y-direction of the end effector's rotation. The movement shown in figure 7.2 are only for this specific direction, and the results are calculated based on this directional data.

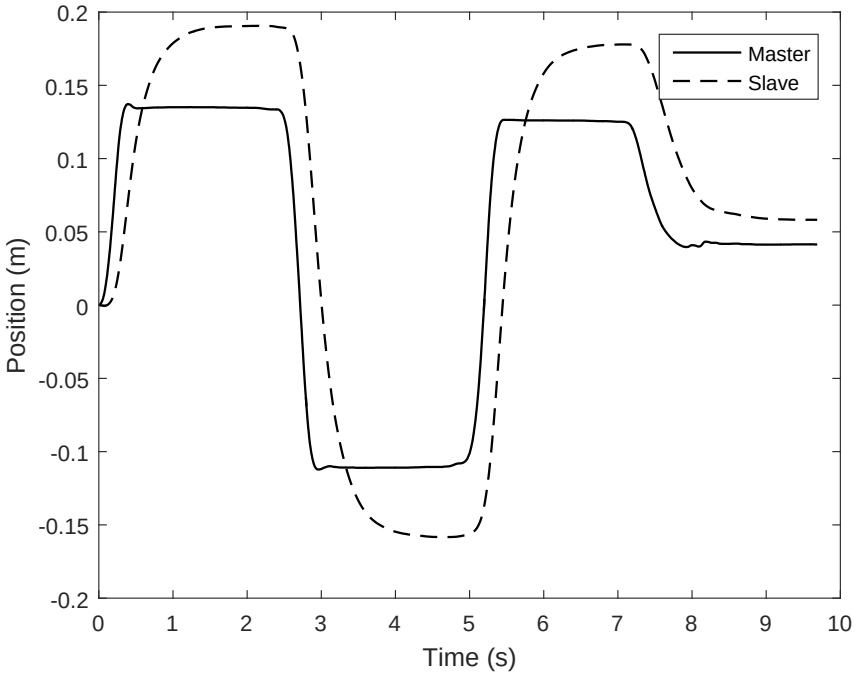

Figure 7.2: Position response of the master in y-direction of the slave when the compliance force controller is not engaged.

In table 7.3 the bandwidth results for the haptic control during free-air movements is shown, both with and without the compliance force controller engaged. The bandwidth of the controller gets worse when using the hybrid control scheme, which is natural since there are more calculations necessary.

	Bandwidth
Without Hybrid Control	66.4 Hz
With Hybrid Control	8.8 Hz

Table 7.3: The bandwidth of the slave/robot position controller

Haptic Force Controller The probe was moved into the phantom at varying amounts of pressure in order to estimate the transfer function of the haptic's force controller. As such we will find the transfer function of the force being sent from the robot and to the haptic controller. The resulting bandwidth of the controller is shown in table 7.4.

	Bandwidth
Haptic Force Controller	14.1 Hz

Table 7.4: The bandwidth of the master/haptic force controller

These movements and bandwidths were measured in z-direction of the end effector, as we are moving downwards into the phantom. Because we have to use the haptic to apply pressure when estimating the haptic force controller, the compliance force controller is turned off.

7.2.2 Compliance Force Control

Below in figure 7.3 the results for the step response from $5N$ to $10N$ are shown. The results have an offset of $0.2N$ on average, which has been removed in figure 7.3 for ease of view. The offset will however be present in any calculations performed when assessing the system.

The master in figure 7.3 is simply a preset value sent to the robot as a setpoint, and is not taken from the haptic device. The slave measurement is gained directly from the force-torque sensor on the slave, and adjusted for the offset.

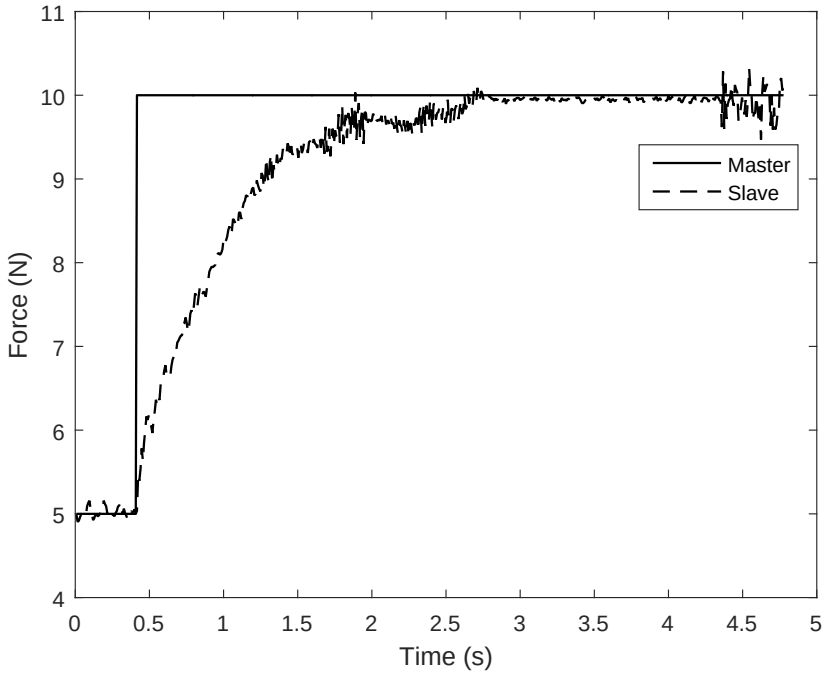

Figure 7.3: The resulting force measured at the slave site when a step is performed in the force setpoint

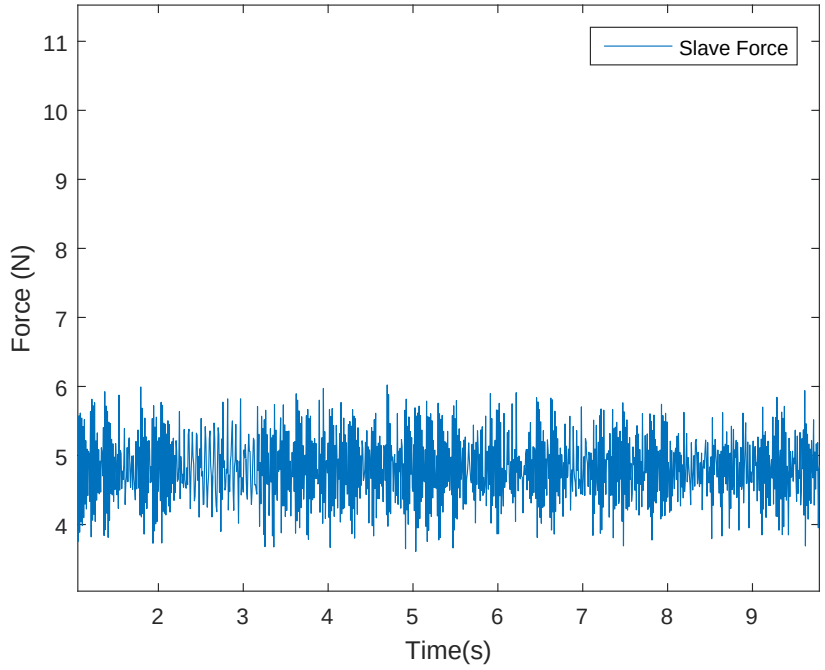

Figure 7.4: The measured force on the slave site with a setpoint of 5N

In table 7.5 the results for the step response are shown. The step response bandwidth is taken from the data shown in figure 7.3, but at this point we use the raw data, and not the one corrected for the offset error. Rise time is defined in [48] as the point where the measured value reaches 95% of the setpoint value.

For calculating the steady state values, a setpoint of $5N$ is used. Figure 7.4 shows part of the dataset, and gives a clear indication of the oscillations present.

Task	Result
Step Response Bandwidth	1.89 Hz
Rise time	129 ms
Steady State Mean value	4.81 N
Steady State SD	0.53 N

Table 7.5: The results from a step response for the master/haptic force control. The steady state Setpoint is 5N

7.2.3 Transparency

By using equation 6.2, and the estimated transfer functions used to get the bandwidth in section 7.2.1, we can now estimate the transparency of the system. To estimate the transparency properly it is important that both transfer functions are estimated using the same directional data.

Therefore an extra step response was performed to get the slave's z-direction response based on the master's movements. As mentioned in section 3.3.3 there are algorithms affecting the slaves velocity when we move in the z-domain. These come into play, although just slightly, even when moving in free-air. This is due to the acceleration of the slave causing disturbances in the force torque sensor. These disturbances do not affect the haptic controller in any noticeable way, but they will worsen the bandwidth of the position controller somewhat. The transparency that is reported below is therefore calculated based on a worst-case scenario.

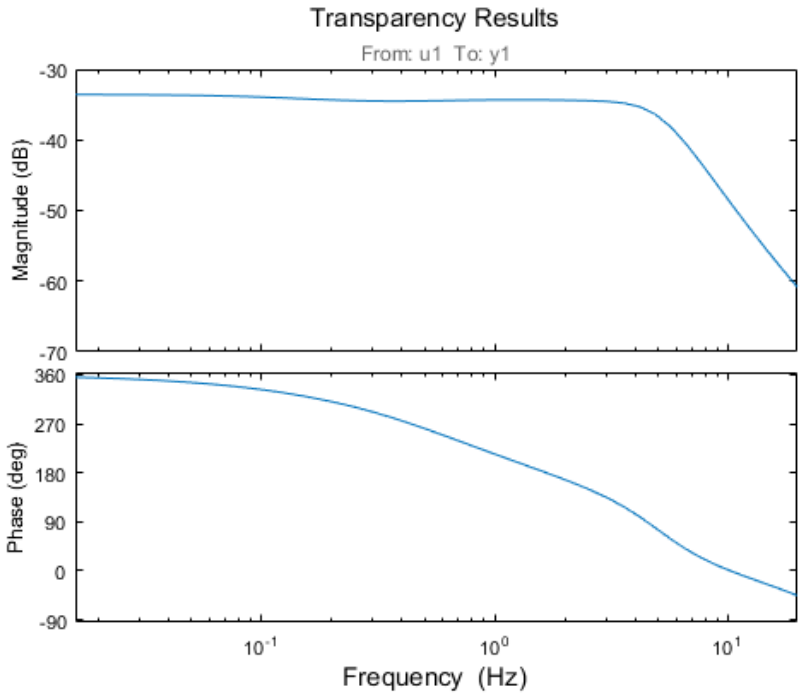

Figure 7.5: The resulting bode plot from the calculated transparency

The calculations used can be seen in equation 6.2. Good transparency is defined by Zandsteeg et al. to be where the magnitude is at $\pm 3dB$ and the phase is at $\pm 45°$ [47]. They reported a transparency of $0.5Hz$ when in contact with fat, which is the closest resemblance to our phantom. Their required transparency bandwidth was $2Hz$ when you take into account both the magnitude and phase limits.

Our *transparency bandwidth* comes out at $4.9Hz$, taken from the bode plot shown in figure 7.5. But from the figure it can be seen that the phase angle is the limiting factor when looking at the requirements for good transparency. Our system has good transparency up to $0.25Hz$, whereafter the phase drops below $45°$. This is worse than what was reported on the system earlier, which was good transparency up to $1.2Hz$ [27].

Chapter 8

User Studies

The plan was to have one single setup for the user study, with one questionnaire. Unfortunately the phantom, described in section 6.1, were destroyed during the studies. This is the reason why there are two test environments set up. For the first test environment no data was gathered from the robot, as the ultrasound image was used to gauge the results. For the second environment data logging was turned on. The answers to the questionnaire, for both environments, are reported in the same bar graph in figure 8.2 and figure 8.3. This is because the questions are the exactly same for both environments. The data gathered for the second test environment, however, is presented by itself in section 8.2.2.

8.1 The Questionnaire

A questionnaire has been made, which is given to every participant. This is in order to gauge both the participant's personal feeling towards using the system, as well as objectively timing the examinations. There is a learning curve to using the system, something that is very clear when comparing my usage, to someone who has not tried the system before. Therefore it is not impossible that any timing improvements could simply be because the participant becomes more comfortable with the system as he or she runs through the tests.

The user studies as a whole will be run as a qualitative testing. This is stated as the best solution for such a system in [49], and comes naturally since we are not after quantitative data at this point in time. Data such as how long the tests take is quantitative in nature, but will only be looked at if there are any huge offsets from the norm. Since the test-pool will be relatively small, running any kind of proper analysis on the timing data is not viable.

What we hope to see is that the use of a hybrid controlling scheme increases the effectiveness and usefulness of the system. It should allow the user to more expertly gauge the position of the objects/lines within the phantom, while not worrying about keeping a steadily applied pressure. During the task it should also help remove some of the necessity for force reflecting, which in turn will make the system feel more stable.

8.1.1 Second Test Environment

A problem quickly became apparent during the user studies. The device used to mount the probe to the robot has some very sharp edges, which are close to the end of the probe. This can be seen in figure 8.1a. As the ultrasound phantom is quite soft, and the users naturally lack experience in controlling the probe, this sharp edge often got pushed into the phantom. This caused greater friction than what the probe by itself would have, and is reflected in the force-feedback as unwanted pressure. It also ripped up the phantom during examinations due to horizontal movement while this

sharp edge was in contact with the phantom. Over a few tests this partially destroyed the phantom's surface, which in turn ruined the ultrasound image at the points where the phantom was ripped open. No data from the robot was recorded during the ultrasound studies, as the focus was to find the reference points in the phantom, and not a reference pressure or precise movement.

A new testing environment was set up, with a slightly adjusted questionnaire. Since we already determined that the ultrasound image was clear when using the system, the second set of tests do not feature an ultrasound phantom. The reason being mostly due to the lack of time necessary to re-design the tool holding the probe. Instead a surface was set up, with two points marked. The first and second setup is shown in figure 8.1. The goal was for the users to attempt a steady movement while maintaining pressure, from one point to the next. They try this both with and without using the hybrid controller, and gauge which control method felt best to use.

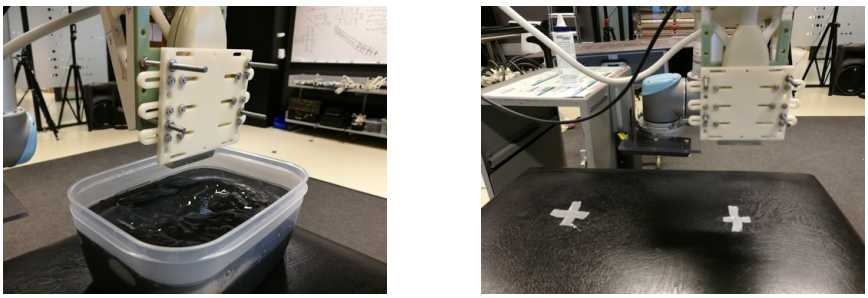

(a) User Studies environment 1 (b) User Studies environment 2

Figure 8.1: The two test setups

The questionnaires in its entirety can be seen in apendix A.

8.2 Results

The results from the questions in the questionnaire are reported as bar graphs. The first and second user in both figures are using the first test environment with the ultrasound phantom. The remaining three are using the second test environment.

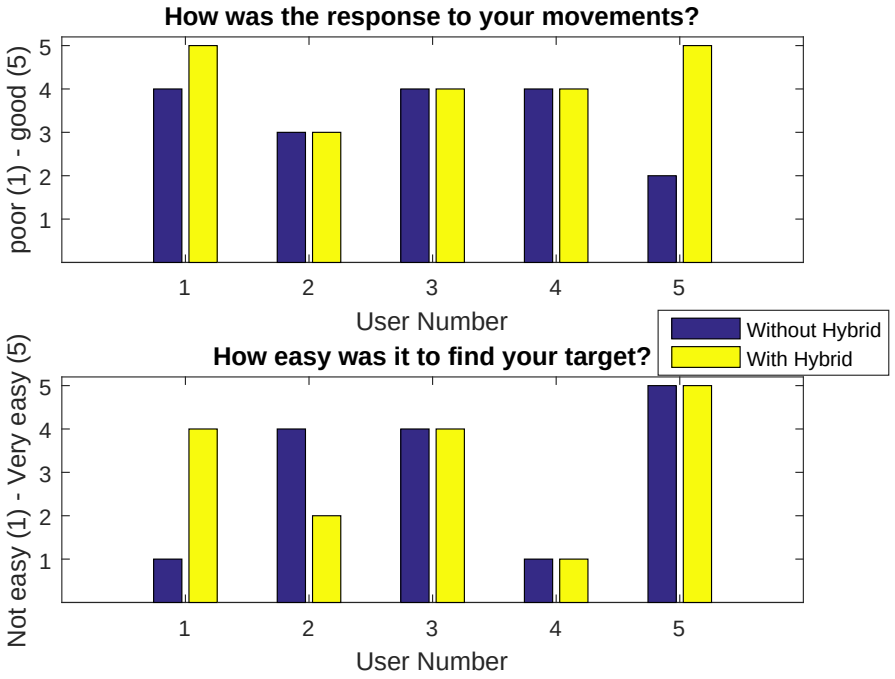

Figure 8.2: Response to the first and second question in the questionnaire.

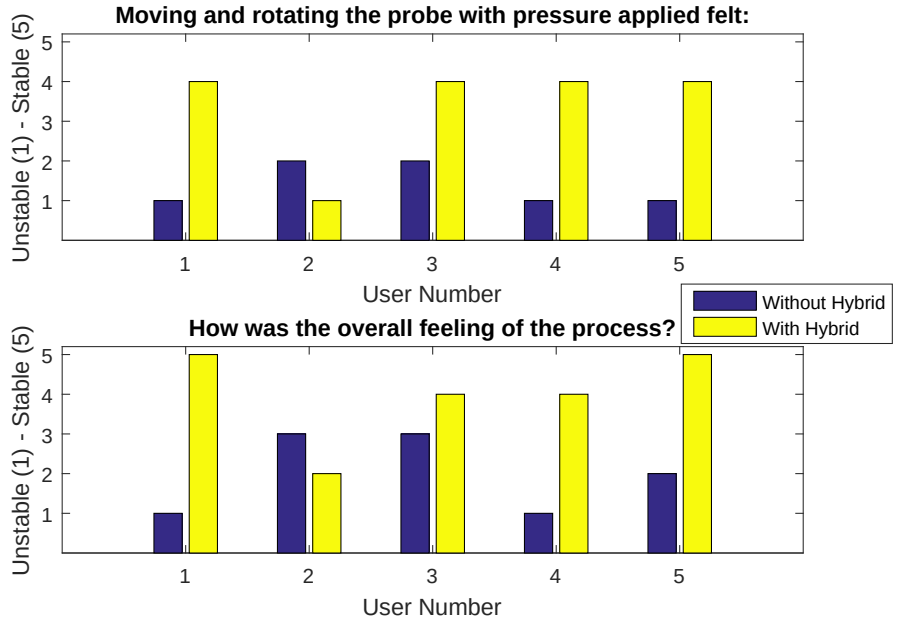

Figure 8.3: Response to the third and fourth question in the questionnaire.

8.2.1 First Test Environment

For the first test environment no user data was gathered. As such the only reported results are from the questionnaires filled out before the

ultrasound phantom was ruined. Since the questions are the same, and simply the exercise changed, both the results from the first and second tests are reported in figure 8.2 and figure 8.3.

8.2.2 Second Test Environment

There were three tests run for the secondary setup, and the results are shown in table 8.1 and 8.2. For all tasks the users were told to look for a pressure of roughly $5 - 10N$. As has been earlier mentioned, finding such a precise pressure is hard, and not really necessary. Therefore what is most important is the stability of the force during the tests. This is because a steady pressure means the ultrasound image also stays still. Figure 8.4 shows the applied force at the slave site for two of the tests when not using hybrid control. The third test was left out to avoid cluttering the graph, but the results were similar. Both figure 8.4 and figure 8.5 show only the timing period for when the probe was moved with an attempt at a steadily applied pressure. Any free-air, or initial positioning movements have been removed.

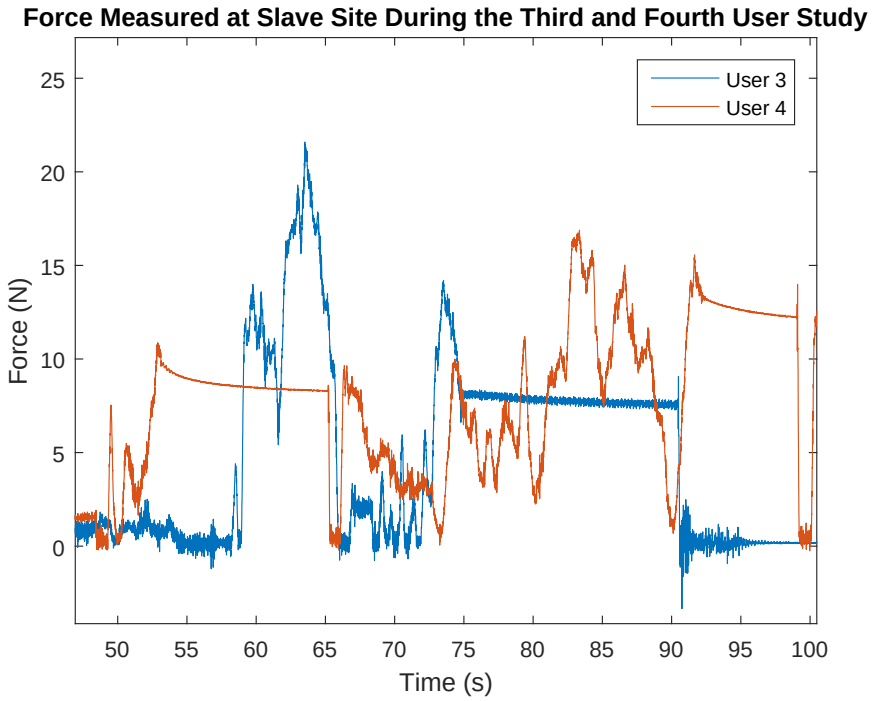

Figure 8.4: Force measurements at slave site as users try to move the probe while maintaining an applied pressure

Figure 8.5 shows the force during the same movement task, but with hybrid control. In this study the movements happened at different timing intervals, and carried a lot of noise, so only one user is shown in the figure. But table 8.2 show the full results from all users of the second test setup.

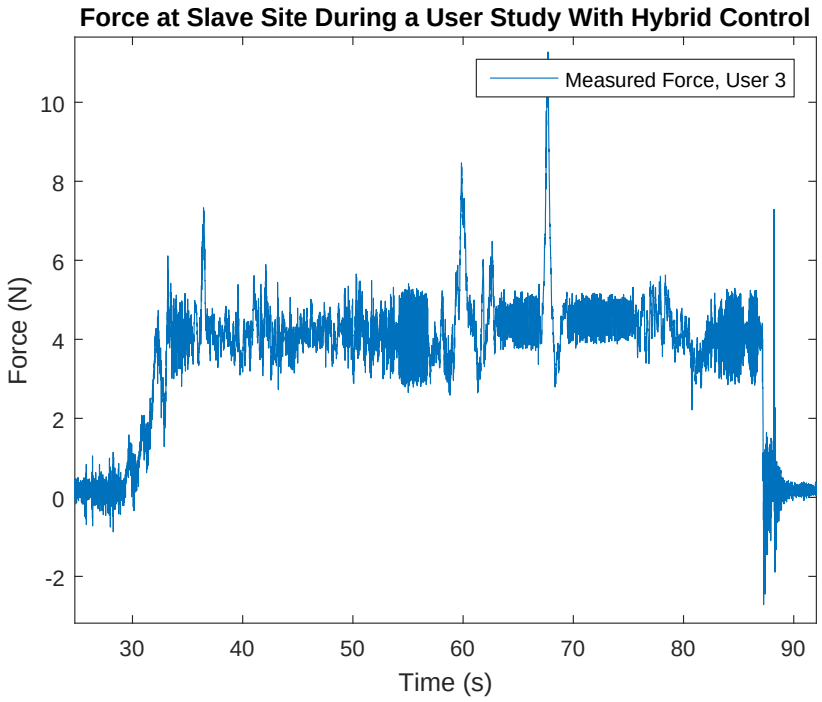

Figure 8.5: Force measurements at slave site as users move the probe with hybrid force control

All values reported in table 8.1 and 8.2 are taken during the movement phase of the test. Any unwanted data while the probe is in free-air has been removed. The standard deviation (SD) assumes $5N$ as the setpoint. The reason the users are numbered $3-5$ is so they follow the same numbering as in figure 8.2 & 8.3.

No Hybrid Controller	
Setpoint to look for	5 N
User 3	
Mean force	5.0 N
SD	4.5
Max force measured	21.5 N
User 4	
Mean force	7.6 N
SD	4.9 N
Max force measured	19.3 N
User 5	
Mean force	3.3 N
SD	3.6
Max force measured	16.3 N

Table 8.1: Questionnaire results when using the second setup without hybrid control

With Hybrid Controller	
Setpoint to look for	5 N
User 3	
Mean force	4.1 N
SD	1.2
Max force measured	11.2 N
User 4	
Mean force	7.6 N
SD	2.0 N
Max force measured	13.4 N
User 5	
Mean force	10.3 N
SD	4.6
Max force measured	16.4 N

Table 8.2: Questionnaire results when using the second setup with hybrid control

Chapter 9

Discussion

9.1 General

The general response of the system is good, and it becomes better to use over time, as you get more familiar with the translation of movement. It is clear that the biggest hurdle at the start is to understand how movement is translated from the master to the slave. Once this becomes clear, and some muscle memory is formed, it is quite intuitive. The users in the study also agree on this. There are improvements that need to be made for the system to become more viable in a real world setting. The most important ones are the force feedback, and the backlash of the haptic controller, which are closely related.

9.2 Force Reflecting

Part of what has made the results for the haptic controller worse is the implementation of the force scaling in section 4.2. While it may be an idea to remove it, in favour of better transparency, the backlash stands as one of the main problems when using the system. This is agreed upon among the people performing the user studies. It may be viable to swap over to a force reflecting controller, and thus solve the problem through improved hardware. But either way, if the system is to continue being used as a force-feedback haptic controlled system this backlash has to be removed, or at the very least filtered out in a more efficient way.

9.3 System Results

9.3.1 Real-Time Performance

Comparing the loop cycle in table 7.1 with what was reported in [27] we see that the cycle time of the controller has not changed. Table 7.2 proves that the control loop time falls well within the cycle time both with and without the force calculations of the hybrid controller engaged. Figure 7.1 also clearly shows this. The loop timing roughly doubles once the force calculations are activated. This is to be expected since the calculations performed are relatively time consuming, but since we stay so well within the control cycle time it does not affect the system's real-time performance.

9.3.2 Forward Flow Haptic Control

It is important to keep in mind that we measured the values at the best-case scenario, which is free-air movement in a sideways direction. The main reason for this is because of how the system responds once pressure is introduced to the force-torque sensor. When used in contact with a soft medium, the slave's movements in relation to the master will change depending on the applied pressure. This change comes from the velocity limiting algorithms discussed in section 3.3.3, and can even come into play if the slave is moved rapidly in the z-domain in free-air. Since we are testing

a position controller scheme it makes more sense to do so in the direction where velocity limits do not come into play, and instead get the master's force controller bandwidth by applying pressure.

From table 7.3 we see that the bandwidth gets worse when using the hybrid controlling scheme. Zandsteeg et al. [47] concludes from their research that haptic control of an ultrasound probe requires good force and position tracking up to $2Hz$. So even though the bandwidth is worse using the hybrid controlling scheme, it is still above this limit. The force tracking of the master device is reported in table 7.4, and also meets these same requirements.

The transparency of the forward flow haptic controller should be improved to account for the maximum respiration bandwidth of $1.5Hz$. The currently implemented force reflecting worsens the bandwidth by making the system slower. As such a better way of doing this should be implemented for the system to work on less specific cases than a phantom.

9.3.3 Compliance Force Control

As mentioned in section 7.2.2 we have an offset of $0.2N$ when attempting to find a setpoint value. In a normal case scenario the operator will move the probe with the haptic controller, which in itself will make it hard to hit a specific force with a $0.2N$ precision. The standard deviation of the controller reported in table 7.5 are also bigger than this value. Taken with the fact that the operator will set the pressure mostly based on the image from the ultrasound, and not necessarily the applied pressure, the small offset is obsolete. In a purely force-controller driven system further steps should be taken to improve these values.

While the force controller works quite well for getting an ultrasound image, it still vibrates while maintaining a force. This can be seen in table 7.5 and figure 7.4, as well as figure 7.3 starting at 4.2 seconds. The standard deviation from the setpoint is quite large, and sits at more than 10% of the mean value. This is due to the oscillations present. The tuning of the compliance force controller is such that the response is good, while the oscillations are sufficiently small. We could remove the oscillations further using the current controller, but this would cause an even more significant drop in the controller's bandwidth, making it slow to respond to any movements at the slave site. Because these oscillations still give a clear ultrasound image, the results are seen as sufficient for our system.

The compliance force controller could need extra work to properly meet certain requirements. De Groote et al. [50] finds that the estimated bandwidth of respiratory motion in a patient is below $1.5Hz$, with its primary component at $0.3Hz$. From the Nyquist sampling theorem the bandwidth of the compliance force controller should thus be double that

of the respiratory bandwidth. If we look at the extremities of $1.5Hz$ our tuning falls short. But based on the primary component we are well above what is necessary. As such, our result bandwidth of $1.89Hz$ from table 7.5 is acceptable, though should be improved so the system will respond well to variances in respiratory motion, such as for example coughing.

9.3.4 Transparency

The transparency results for our system falls short of the requirements in [47], which were $2Hz$. They themselves also reported poor results based on their requirements. Even so, from a user's point of view our system still feels reactive, and changes in the applied pressure or movement will still be felt, and is mostly limited to whether or not the haptic controller's actuators are fully saturated, or close to it.

When performing the step response in z-direction the velocity limiting factors all come into play, even while in free air. Most prominent is probably the new low-pass cutoff frequency, and the force-scaling. These two algorithms cause the system to feel better to use for the operator, and reduces the backlash, as well as still giving a seemingly good response to pressure changes. But as seen in the resulting transparency in figure 7.5, a question is raised of whether or not they should be changed further, or removed entirely in order to maintain a better transparency.

9.4 Hybrid Controller

The hybrid controller has been implemented, and functions as expected from a user perspective. But from a system performance perspective each part of the controller does fall a bit short of the required specifications. It stands as a proof of concept, and can be seen in theory as a very viable option in controlling a robot during ultrasound examinations. But for it to actually be used successfully, parts of the system will need improvements.

The parts that need to be improved, such as the transparency of the haptic controller, or the bandwidth of the compliance force controller, are all individual pieces. These can be improved as standalone parts of the system. As such, if the haptic controller alone, or compliance force controller is improved, this will be reflected in the hybrid controller. This allows for continuous development of these individual parts without worrying too much about how they are combined. Both controllers can by themselves also be used to implement other functions or hybrid controllers for the system.

The way the hybrid controller has been implemented also allows for an easily interchangeable force-controlling scheme. This makes it easy to try out different force controllers by simply changing the force input of the hybrid controller. All in all the position-force hybrid control is a good

pairing of a master controlled system that incorporates an internal force controller on the slave site.

9.5 User Studies

Any timing measurements from the studies proved to be irrelevant since there were not big deviations, and too few tests. In figure 8.2 we see the results from the first and second question in the questionnaire. There are not a whole lot of improvements reported, but that is not necessarily a bad thing. For the first question this tells us that the system as a whole functions and responds well, even when the slightly worse bandwidth of the hybrid controller is introduced.

For the second question we see no changes in the last three participants. These participants were told to simply align the robot with the points seen in figure 8.1b. As such, no real changes are going to come into play whether the hybrid controller is engaged or not.

For the first two, which were the ones attempting to find points within the ultrasound phantom, there are some differences. The first user reports a substantial increase in the ease of finding the points when using the hybrid controller. This was credited to the lack of backlash after locking in the force with the hybrid controller.

The second user on the other hand, reports a decrease. Upon further inquiry this was said to be due to the behaviour of the slave once the hybrid controller was engaged. The lack of any z-directional movement caused the rotation of the slave to be less intuitive, as z-movement in the master would be translated into rotation in the slave. This is also reflected in the user's response to the third and fourth question.

For the rest of the users, we see improvements in the third and fourth question, shown in figure 8.3. These are probably the most important ones for this thesis, as they show an overall improvement in the use of the system. Every user has reported that the backlash is a big problem, and the improvements reported in question three is mostly credited to the lack of backlash, after the hybrid controller is engaged and takes care of the z-directional force.

9.5.1 Secondary Test Data

Finding a very precise pressure when using a haptic device is hard. Therefore a precision of exactly $5N$ of pressure is deemed to be less important in this study, than the stability of the applied pressure while the user moves the probe around. This is because a steady pressure results in a steady ultrasound image.

Without Hybrid Control The results shown in figure 8.4 prove that there are huge fluctuations in the applied force when attempting to hold a pressure and move the probe without using a hybrid controller. The seemingly steady pressure at around 75-90 seconds for the first user in figure 8.4 is simply the user letting go of the button on the haptic controller. This locks the robot in place, naturally causing a constant pressure, though not a dynamic one. From the questionnaire the result reflect what the users felt. The force feedback was too jittery to be properly useful, especially when moving the probe along a surface. The backlash is a hindrance that makes the feedback seem like it is just in the way of the movement operation. All users reported that this would likely get better with more training, as they would become more used to handling it. But even so, their response stands as an indicator that the force reflecting, and force-feedback in general needs improvement.

With Hybrid Control Figure 8.5 is basically a repeat of what we see in figure 7.4. This is a good thing, as it means the compliance force controller works well even when moving the probe along a surface, and not just when held in place. The spikes in force, seen at roughly $60s$ and $80s$ in figure 8.5, come from rapid movements or rotations of the master. This causes a sudden increase in the measured force, as the slaves rotation causes extra friction, or extra downwards pressure since the probe is not a symmetrical shape.

Table Results From table 8.1 we see that for all users the mean value of the applied force is not far from $5N$. But figure 8.4 proves that the mean value does not represent good control of the probe. The fact that it gets close is because the actual value is in the range of $0 - 10N$. The standard deviation from the setpoint proves that the fluctuations are relatively big. Compared to the first and second user test with hybrid control the improvements in standard deviation are quite clear.

The mean force for the tests using the hybrid control are also off the mark. This is to be expected, as finding an exact amount of pressure is really hard using this system. The maximum force applied also reflects this. As the users attempt to find the pressure, they often overshoot the target at first. But the standard deviation is a big improvement. It goes to show that even while moving the probe around, the hybrid control allows for a much more steady force application. In a case where a good ultrasound image is found, this allows for the image to stay clear as the user moves the probe around. This is more important than an exact amount of force for our intended use. For the third user, the mean force and standard deviations are worse again during hybrid control. This is because the user chose to lock the force controller at roughly $10N$. But even in this case the stability and ease of use was reported to be very much improved.

Chapter 10

Conclusion

The goal of this thesis was to make a system capable of combining a radiologist's expertise in ultrasound examinations, with a robot's precision, and assistance capabilities. This would be done by combining an external master haptic control with force feedback, and an internal force control for the slave robot. It was built upon a previous system implemented by Mathiassen [27] and Fjellin [7] making use of a UR-5 robot and a Phantom Omni haptic controller. By using a haptic control and an automated force control the radiologist should be able to control the robot which holds the probe, find a clear ultrasound image, and then have the force controller keep the currently applied pressure. This would give a clear and steady ultrasound image, and allow the radiologist to fine-tune the position of the probe without continuously applying pressure.

This goal has been reached, and the hybrid position-force controller has been implemented in a working fashion, with the help of a pedal to turn the compliance force controller on or off. The user is able to rotate the probe and move it around while the force controller takes care of the applied pressure on the slave site. The user studies show that the introduction of the hybrid controller improves the ease of using the system, while still keeping it responsive to the master's movements.

The controller has been implemented in a way that allows it to maintain the earlier measured real-time requirements of the system. Unfortunately the system's transparency turned out to be worse, and the bandwidth of the compliance force controller falls short of what is deemed necessary to allow for disturbances in a patient's respiration, such as coughing. As such the hybrid controller needs some improvements in order to meet the requirements set for such a system.

Some improvements have been made to the previously implemented haptic controller. This was in order to reduce the amount of backlash from the haptic controller when the slave comes into contact with a medium. These improvements turned out not to be sufficient. While the results did improve, the backlash is still, based on user feedback, one of the main downfalls of the system.

10.1 Future Work

10.1.1 Compliance Force Control

As has been mentioned in section 9.3.3 some improvements should be made to the internal compliance force controller to increase its bandwidth, and account for variances in the respiratory system of a patient. Another improvement to this force controller would be to pre-load a couple of different tuning parameters based on what kind of examination is taking place. This is because a force controller tuned for soft tissue is not going to

work as well with hard tissue, where a higher amount of pressure may be necessary.

Currently the controller can be seen as a PI controlling scheme, where the dampening factor is the I-term. It might be possible to introduce a derivative term to this controller. This could allow us to tune the controller differently, so that it has a low amount of oscillations when holding a given force, and still reacts to rapid pressure changes.

10.1.2 Backlash Mitigation

The hybrid controller has been implemented in part successfully. It is clear that it requires some improvements to be optimal. From a user's standpoint the most important part is seemingly to get a better force reflection in place. This could be achieved multiple ways, for example by using optical sensors that keep track of when the probe will come into contact with the patient. It could also to some extent be achieved with a better force-reflecting algorithm, even though that is somewhat limited to the timing of the control loop, and system in general. It could be viable to try out a different kind of hardware, that has integrated force reflection, as described in section 2.4. This would give an indication of just how good the improvements would be, and whether or not the system should be made more specific, with such a haptic controller in mind. Force reflecting is after all a very important part of having a stable system for these kinds of application, both at the master and slave site.

10.1.3 Force Feedback Dissipation

Removing the pressure instantly when activating the hybrid force controller can cause a sudden jolt in movement. This happens since the feedback disappears while the radiologist still applies pressure to the controller. Leaving the force-feedback on at all times, would cause discomfort for the operator, and make the entire procedure feel awkward and hard to control. A better solution is to slowly dissipate the force-feedback until it becomes zero for the z-direction pressure. This would allow the radiologist to slowly ease off on the pressure he or she applies to the controller, in a controlled and natural fashion.

Another important matter is how the force-feedback should be reintroduced once the pedal is pressed again. It could work out to scale the pressure back up, in the same way as it was scaled down. When the pedal is pressed the second time, the internal force-control will be disabled, and the external haptic controller will again be allowed to move the probe in all directions. While the force-feedback does not return instantly, the radiologist will be able to move the probe away from the patient right away. This is important in case the pressure needs to be relieved in an instant due to, for example, discomfort for the patient. An issue may arise in that the radiologist could apply even more pressure without realising it. But this

should not be a big problem due to the newly implemented force-limit, and already existing velocity limiting algorithms.

It is hard to determine the best way to do this in any other way than to have people test the different solutions to the problem. As such a more in-depth user study would be preferable in order to figure out the best way to tackle the problem.

10.1.4 Improved User Interface

While the information shown in the labview front panel is useful for setting up the system before starting an examination, it could be changed to show the necessary information more clearly. Currently the user has to look at three places during an examination. The front panel, the robot and the ultrasound machine. Making a new user interface which combines data from the front panel with the ultrasound image could be useful. A better form of force visualisation would also be very helpful, as the current graph in the front panel is a bit hard to read. A user during the user studies mentioned how it would be nice to have an indication of the applied force on the robot itself. This could be done either as a numerical display, or a simple color coded bar. Another way to implement this would be to introduce augmented reality to the system. This could allow for the necessary information to float in the air next to the robot while performing an examination.

10.1.5 Hybrid controller

The position controller should be integrated with the compliance matrix, so the matrix can be used to determine which degrees of freedom should be controlled with the haptic device. Currently this is only predetermined in the code. By setting up the hybrid controller to properly make use of the compliance matrix the entire architecture becomes more generalised. This would allow for either the force controller, or the position controller to be swapped out for a better one more easily, as long as the input to the hybrid architecture stays the same.

Bibliography

[1] S. E. Salcudean, G. Bell, S. Bachmann, W. H. Zhu, P. Abolmaesumi, and P. D. Lawrence, "Robot-Assisted Diagnostic Ultrasound - Design and Feasibility Experiments," in *Medical Image Computing and Computer-Assisted Intervention - MICCAI'99*, vol. 1679 of *Lecture Notes in Computer Science*, pp. 1062–1071, University of British Columbia, Department of Electrical and Computer Engineering, 1999.

[2] H. E. Vanderpool, E. A. Friis, B. S. Smith, and K. L. Harms, "Prevelance of Carpal Tunnel Sydrome and Other Work-Related Musculoskeletal Problems in Cardiac Sonographers," *Journal of Occupational Medicine*, vol. 35, pp. 604 – 610, June 1993.

[3] N. Enayati, E. D. Momi, and G. Ferrigno, "Haptics in Robot-Assisted Surgery: Challenges and Benefits," *IEEE Reviews in Biomedical Engineering*, vol. PP, no. 99, pp. 1–1, 2016.

[4] "Robotic Surgery: da Vinci Versus The Ideal." Article at http://www.informationweek.com/healthcare/clinical-information-systems/robotic-surgery-da-vinci-versus-the-ideal/d/d-id/1112732.

[5] B. T. Bethea, A. M. Okamura, M. Kitagawa, T. P. Fitton, S. M. Cattaneo, V. L. Gott, W. A. Baumgartner, and D. D. Yuh, "Application of Haptic Feedback to Robotic Surgery," *Journal of laparoendoscopic & advanced surgical techniques. Part A*, vol. 14, pp. 191–195, June 2004.

[6] "PHANTOM OMNI - Sensable," Sept. 2016. Technical specification and product details available at http://www.dentsable.com/haptic-phantom-omni.htm.

[7] J. E. Fjellin, *Design of a bilateral master-slave system with haptic feedback for ultrasound examinations*. Master Thesis, University of Oslo, 2013.

[8] A. M. Priester, S. Natarajan, and M. O. Culjat, "Robotic Ultrasound Systems in Medicine," *Transactions on Ultrasonics, Ferroelectrics, and Frequency Control*, vol. 60, pp. 507 – 523, Mar. 2013.

[9] A. Gourdon, P. Poignet, G. Poisson, P. Vieyres, and P. Marche, "A New Robotic Mechanism for Medical Application," *Advanced Intelligent Mechatronics*, pp. 33 – 38, Sept. 1999.

[10] P. Arbeille, J. Ayoub, V. Kieffer, P. Ruiz, B. Combes, A. Coitrieux, P. Herve, S. Garnier, B. Leportz, E. Lefbvre, and F. Perrotin, "Realtime Tele-operated Abdominal and Fetal Echography in 4 Medical Centres, from one Expert Center, using a Robotic Arm & ISDN or Satellite Link," *Automation, Quality and Testing, Robotics, 2008*, vol. 1, pp. 45 – 46, May 2008.

[11] F. Courreges, P. Vieyres, and R. S. H. Istepanian, "Advances in Robotic Tele-echography Services - The OTELO System," *Engineering in Medicine and Biology Society, 2014.*, vol. 2, pp. 5371 – 5374, Jan. 2004.

[12] A. Vilchis, J. Troccaz, P. Cinquin, K. Masuda, and F. Pellissier, "A new robot architecture for tele-echography," *IEEE Transactions on Robotics and Automation*, vol. 19, pp. 922–926, Oct. 2003.

[13] E. Degoulange, L. Urbain, P. Caron, S. Boudet, J. Gariepy, J. L. Megnien, F. Pierrot, and E. Dombre, "HIPPOCRATE: an intrinsically safe robot for medical applications," in *, 1998 IEEE/RSJ International Conference on Intelligent Robots and Systems, 1998. Proceedings*, vol. 2, pp. 959–964 vol.2, Oct. 1998.

[14] "Robotic-assisted surgical technology by Intuitive Surgical." Information available at https://www.intuitivesurgical.com/.

[15] S. Shimachi, S. Hirunyanitiwatna, Y. Fujiwara, A. Hashimoto, and Y. Hakozaki, "Adapter for contact force sensing of the da Vinci robot," *The international journal of medical robotics + computer assisted surgery: MRCAS*, vol. 4, pp. 121–130, June 2008.

[16] A. M. Tahmasebi, P. Abolmaesumi, and K. Hashtrudi-Zaad, "A Haptic-based Ultrasound Training/Examination System (HUTES)," in *Proceedings 2007 IEEE International Conference on Robotics and Automation*, pp. 3130–3131, Apr. 2007.

[17] R. Antonello, O. A. Daud, R. Oboe, and E. Grisan, "Stability of a telerobotic manipulation system with proximity Based haptic feedback," in *IECON 2012 - 38th Annual Conference on IEEE Industrial Electronics Society*, pp. 2786–2792, Oct. 2012.

[18] T. Sansanayuth, I. Nilkhamhang, and K. Tungpimolrat, "Teleoperation with inverse dynamics control for PHANToM Omni haptic device," in *2012 Proceedings of SICE Annual Conference (SICE)*, pp. 2121–2126, Aug. 2012.

[19] K. J. Kuchenbecker and G. Niemeyer, "Modeling Induced Master Motion in Force-Reflecting Teleoperation," in *Proceedings of the 2005 IEEE International Conference on Robotics and Automation*, pp. 348–353, Apr. 2005.

[20] I. G. Polushin, P. X. Liu, and C.-H. Lung, "Stability of bilateral teleoperators with projection-based force reflection algorithms," in

2008 IEEE International Conference on Robotics and Automation, pp. 677–682, May 2008.

[21] D. J. F. Heck, A. Saccon, and H. Nijmeijer, "A two-layer architecture for force-reflecting bilateral teleoperation with time delays," in *2015 54th IEEE Conference on Decision and Control (CDC)*, pp. 1509–1514, Dec. 2015.

[22] J. Qu, J. Li, L. Zhang, K. Liang, N. Lv, and H. Su, "Design of a novel force-reflecting haptic device for minimally invasive surgery robot," in *2013 ICME International Conference on Complex Medical Engineering*, pp. 357–362, May 2013.

[23] D. A. McAffee, E. R. Snow, and W. T. Townsend, "Force reflecting hand controller," Mar. 1993. Klassifisering i USA 414/5, 414/7; Internasjonal klassifisering B25J3/04, B25J13/02; Patentklassifisering B25J3/04, B25J13/025; European Classification (ECLA) B25J3/04, B25J13/02.

[24] M. W. Spong, S. Hutchinson, and M. Vidyasagar, *Robot Modeling And Control*. John Wiley & Sons Inc, 2005.

[25] F. L. Lewis, C. T. Abdallah, and D. M. Dawson, *Control of robot manipulators*. Macmillan Pub. Co., 1993. Google-Books-ID: _TVSAAAAMAAJ.

[26] H.-J. Hsieh, C.-C. Hu, T.-W. Lu, H.-L. Lu, M.-Y. Kuo, C.-C. Kuo, and H.-C. Hsu, "Evaluation of three force-position hybrid control methods for a robot-based biological joint-testing system," *BioMedical Engineering OnLine*, vol. 15, June 2016.

[27] K. Mathiassen, J. E. Fjellin, K. Glette, P. K. Hol, and O. J. Elle, "An Ultrasound Robotic System Using the Commercial Robot UR5," *Biomedical Robotics*, 2016.

[28] Y. Yao, Q. Huang, Y. Peng, and T. Oiwa, "Hybrid position, posture, force and moment control with impedance characteristics for robot manipulators," in *2011 IEEE International Conference on Mechatronics and Automation*, pp. 2129–2134, Aug. 2011.

[29] H. Fujie, K. Mabuchi, S. L. Woo, G. A. Livesay, S. Arai, and Y. Tsukamoto, "The use of robotics technology to study human joint kinematics: a new methodology," *Journal of Biomechanical Engineering*, vol. 115, pp. 211–217, Aug. 1993.

[30] S. Herrmann, M. Kaehler, R. Souffrant, R. Rachholz, J. Zierath, D. Kluess, W. Mittelmeier, C. Woernle, and R. Bader, "HiL simulation in biomechanics: a new approach for testing total joint replacements," *Computer Methods and Programs in Biomedicine*, vol. 105, pp. 109–119, Feb. 2012.

[31] N. Koizumi, S. Warisawa, M. Mitsuishi, and H. Hashizume, "Automatic Control Switching according to Diagnostic Tasks for a Remote Ultrasound Diagnostic System," in *The First IEEE/RAS-EMBS International Conference on Biomedical Robotics and Biomechatronics, 2006. BioRob 2006.*, pp. 1141–1148, Feb. 2006.

[32] M. Hasan, "A robust real time position and force (hybrid) control of a robot manipulator in presence of uncertainties," in *Proceedings of IEEE International Conference on Multisensor Fusion and Integration for Intelligent Systems, MFI2003.*, pp. 38–43, July 2003.

[33] D. Jeon and M. Tomizuka, "Learning hybrid force and position control of robot manipulators," *IEEE Transactions on Robotics and Automation*, vol. 9, pp. 423–431, Aug. 1993.

[34] M. C. Yip and D. B. Camarillo, "Model-Less Hybrid Position/Force Control: A Minimalist Approach for Continuum Manipulators in Unknown, Constrained Environments," *IEEE Robotics and Automation Letters*, vol. 1, pp. 844–851, July 2016.

[35] "Universal Robots," 2015. Technical specifications and safety certificate available at http://www.universal-robots.com/products/ur5-robot/.

[36] "SI-65-5 Datasheet – ATI Industrial Automation – Gamma | Engineering360."

[37] "Robotiq FT Sensor on ROS Industrial," Dec. 2016. Technical specifications available at http://robotiq.com/products/robotics-force-torque-sensor-ft-150/ft-sensor-on-ros-industrial-force-torque-sensor/.

[38] "Armadillo: C++ linear algebra library," Aug. 2016. Information available at http://arma.sourceforge.net/.

[39] T. Timm, "UR Modern Driver." The driver can be found and downloaded at https://github.com/ThomasTimm/ur_modern_driver.

[40] "Xenomai – Real-time framework for Linux," Aug. 2016. Information available at http://xenomai.org/.

[41] C. G. Atkeson, C. H. An, and J. M. Hollerbach, "Estimation of Inertial Parameters of Manipulator Loads and Links," *The International Journal of Robotics Research*, vol. 5, pp. 101–119, Sept. 1986.

[42] E. Naerum and B. Hannaford, "Global transparency analysis of the Lawrence teleoperator architecture," in *IEEE International Conference on Robotics and Automation, 2009. ICRA '09*, pp. 4344–4349, May 2009.

[43] B. Siciliano, L. Sciavicco, L. Villani, and G. Oriolo, *Robotics: Modelling, Planning and Control*. Advanced Textbooks in Control and Signal Processing, Springer London.

[44] K. Boman, M. Olofsson, J. Forsberg, and S.-k. Boström, "Remote-Controlled Robotic Arm for Real-Time Echocardiography: The Diagnostic Future for Patients in Rural Areas?," *Telemedicine and e-Health*, vol. 15, pp. 142–147, Mar. 2009.

[45] J. M. Sackier and Y. Wang, "Robotically assisted laparoscopic surgery," *Surgical Endoscopy*, vol. 8, pp. 63–66, Jan. 1994.

[46] E. L. Madsen, G. R. Frank, and F. Dong, "Liquid or Solid Ultrasonically Tissue-Mimicking Materials with Very Low Scatter," *Ultrasound in Medicine & Biology*, vol. 24, pp. 535–542, May 1998.

[47] C. J. Zandsteeg, D. J. H. Bruijnen, and M. J. G. van de Molengraft, "Haptic tele-operation system control design for the ultrasound task: A loop-shaping approach," *Mechatronics*, vol. 20, pp. 767–777, Oct. 2010.

[48] W. S. Levine, *The Control Handbook*. second edition ed., 1996.

[49] J. Lazar, J. H. Feng, and H. Hocheiser, *Research Methods In Human-Computer Interaction*. John Wiley & Sons Inc, 2010.

[50] A. D. Groote, M. Wantier, G. Cheron, M. Estenne, and M. Paiva, "Chest wall motion during tidal breathing," *Journal of Applied Physiology*, vol. 83, pp. 1531–1537, Nov. 1997.

Appendices

Appendix A

The Questionnaire

Questionnaire

About you

1. **Profesion:** _____
2. **How old are you?** _____
3. **Have you tested this system before?** □ Yes □ No
4. **Have you ever tested another robot-assisted Haptic system?** □ Yes □ No

How would you rate your experience in conventional ultrasound examinations

None □—□—□—□—□ Experienced

1 The task

In this experiment you will be orienting the probe towards a given point. Once found, you will first attempt to find a pressure of $5N$ using nothing but the haptic controller. While maintaining pressure you will move the probe to the other marked out location, and rotate it 90° once there.

After this first run, you will do the same thing, but once you find the correct pressure you will press the pedal. Doing this will engage an internal force-controller on the robot, allowing it to take care of the applied pressure.

After each of the two tests, please answer the questions below.

2 Teleoperating with only haptic control

Was the response to your movements:

Poor □—□—□—□—□ Good ,

How easy was it to find your target?

Not easy □—□—□—□—□ Very easy

How did moving and rotating the probe feel while maintaining pressure?

Unstable □—□—□—□—□ Stable

How was the overall feeling of the process?

Unstable □—□—□—□—□ Stable

3 Using the hybrid controller

Was the response to your movements when the force was locked:

Poor □—□—□—□—□ Good ,

How easy was it to find your target?

Not easy □—□—□—□—□ Very easy

How did moving and rotating the probe feel while maintaining pressure?

Unstable □—□—□—□—□ Stable

How was the overall feeling of the process?

Unstable □—□—□—□—□ Stable

4 General

In a few words, what would you say worked well in this system?

What would be most important to improve for you to use it?

Would a longer training period have made the system better for you to use?

5 Objective observations

Filled out by the observer.

Just haptic control

5. Time spent: _____

Accuracy: Poor □—□—□—□—□ Perfect

Hybrid controller with full force-feedback

6. Time spent: _____

Accuracy: Poor □—□—□—□—□ Perfect